The Jabal Akhdar Dome in the Oman Mountains: evolution of a dynamic fracture system

E. GOMEZ-RIVAS*, P. D. BONS*, D. KOEHN**, J. L. URAI***, M. ARNDT***, S. VIRGO***, B. LAURICH***, C. ZEEB****, L. STARK* and P. BLUM****

* Department of Geosciences, Eberhard Karls University Tübingen, Germany; enrique.gomez-rivas@uni-tuebingen.de

** School of Geographical and Earth Sciences, University of Glasgow, Glasgow, United Kingdom

*** Structural Geology, Tectonics and Geomechanics, RWTH Aachen University, Germany

**** Institute for Applied Geosciences (AGW), Karlsruhe Institute of Technology (KIT), Germany

ABSTRACT. The Mesozoic succession of the Jabal Akhdar dome in the Oman Mountains hosts complex networks of fractures and veins in carbonates, which are a clear example of dynamic fracture opening and sealing in a highly overpressured system. The area underwent several tectonic events during the Late Cretaceous and Cenozoic, including the obduction of the Samail ophiolite and Hawasina nappes, followed by uplift and compression due to the Arabia-Eurasia convergence. This study presents the results of an extensive tectonic survey, and correlates subseismic-scale structures in Jabal Akhdar (faults, fractures, veins and stylolites) with the main tectonic events in the Northeastern Arabian plate. As some of the studied formations host large oil reserves in neighboring areas, determining the relative timing of these events in the exhumed rocks is important to understand hydrocarbon distribution and fracture patterns in these reservoirs. The formation of early veins and stylolites in the Oman Mountains is followed by top-to-the-South layer-parallel shearing that may be associated with the obduction of the Samail and Hawasina nappes. This compressional tectonic event is followed by normal (dip-slip) to oblique-slip faults and veins. Top-to-the-Northeast layer-parallel shearing, which corresponds to the first stage of exhumation of the autochthonous rocks offsets these structures. Our new data indicate that this first phase of events is overprinted by complex strike-slip networks of veins and fractures, as well as by the reactivation and onset of seismic-scale faults. Strike slip structures belong to three distinct events. The first one

(NW-SE-oriented compression) is probably associated to the oblique collision of the Indian plate against the Arabian platform during the Late Campanian to the Mid Eocene. The second event (E-W-oriented compression) is likely to have been formed during the Late Oligocene-Middle Miocene during uplift. The last event (NE-SW-oriented compression) probably took place during the Miocene-Pliocene. Structures of the first two strike-slip events have the same orientation as seismic-scale faults observed in the subsurface of Oman and Abu Dhabi. In addition, increasing vein intensity towards the top of the autochthonous formations in the Oman mountains, as well as the small angle between conjugate vein sets, indicate that high fluid pressures that are thought to be present during strike-slip deformation.

INTRODUCTION

Subseismic-scale fractures, veins and stylolites play a fundamental role on controlling fluid flow in the upper crust (e.g., Cox and others, 2001; Koehn and others, 2007), they are proxies for paleostress directions (e.g., Van Noten and others, 2011; 2012), deformation kinematics, fluid pressures (e.g., Jaeger and others, 2007) and can be used to unravel the geological history of an area. Mineralogy and geochemistry of vein-filling minerals and properties of fluid inclusions provide significant information on the conditions during vein formation (temperature, depth, pressure) as well as on the fluid properties (composition, origin) (e.g. Bons and others, 2012 and references therein). Stylolites can be utilized to determine stress directions and magnitudes (Ebner and others, 2010; Koehn and others, 2012) and layer-parallel stylolites that developed as a consequence of sediment load can provide estimates of the burial depth at which they formed (e.g. Koehn and others, 2007; Koehn and others, 2012).

Fluid overpressure causes a decrease of effective stress, enhances rock failure (Hubbert and Rubey, 1959; Etheridge, 1983; Jaeger and others, 2007) and is often found in sedimentary basins (e.g. Law and others, 1998). Abnormal pressures, which are of importance for hydrocarbon exploration and production, may be due to disequilibrium compaction, fluid volume expansion, gas generation or thermal expansion, formation of cements, transfer of fluids from overpressured rocks, hydraulic head and hydrocarbon buoyancy (e.g., Swarbrick and Osborne,

1998; Nordgard Bolas and others, 2004). Although overpressured reservoirs are typical for low-permeability shale-like rock (Law and others, 1998) they can also occur in other sedimentary rocks, like carbonates.

The Mesozoic succession of the Jabal Akhdar dome in the Oman Mountains (Glennie and others, 1974; Breton and others, 2004; Glennie, 2005; Searle, 2007) is an example of a highly dynamic thermal, hydraulic and mechanical system (Holland and others, 2009a), where complex networks of fractures, veins and stylolites are well exposed and fluid pressures were interpreted to have been close to lithostatic (Hilgers and others, 2006; Holland and others, 2009a; 2009b). Some of the Early Cretaceous formations in neighbouring areas host large oil reserves so that studying the Jabal Akhdar area is not only important in order to unravel fracture and vein network development, but, despite differences in metamorphic and tectonic history, may also help to understand subseismic-scale fracture distributions in the oil fields of the NE Arabian plate.

Based on previous studies (Hilgers and others, 2006; Holland and others, 2009a; 2009b) we have carried out a detailed structural field study in the exhumed Jurassic and Cretaceous rocks of the Autochthonous B succession in the Jabal Akhdar area (Oman Mountains; figs. 1, 2). Our new data show that strike-slip deformation played a more important role in the area than previously thought. Holland and others (2009a) and Holland and Urai (2010) proposed that veins and fractures formed in a high-pressure cell. Here we evaluate this hypothesis in the context of a complex system of fractures that is constantly opening and resealing during numerous tectonic events coupled with high fluid pressures in a changing stress field.

The presented study also provides an example of how the large-scale tectonic evolution of a complex area can be unraveled from the analysis of outcrop-scale structures like faults, fractures, veins and stylolites. Moreover, we illustrate how such a study can complement the results of seismic surveys, by providing information at the small-scale that is undetectable in seismic profiles.

GEOLOGICAL SETTING

The Jabal Akhdar dome is located in the central part of the Oman Mountains and extends for 700 km from the Musandam Peninsula in the northwest to the Batain coast in the southeast. The Oman Mountains are part of the Alpine-Himalayan chain, and were formed during several tectonic events, including a northeast-directed subduction of the Arabian below the Eurasian plate, and further exhumation, transtension, uplift and doming (fig. 1; e.g. Breton and others, 2004 and references therein). According to Searle and Malpas (1980), Pearce and others, (1981), Searle and Malpas (1982) and Lippard (1983), intra-oceanic subduction was initiated in the Cenomanian and continued throughout the early Campanian. This process gave rise to the obduction and emplacement of two major nappe units: (a) the volcano-sedimentary Hawasina and Sumeini nappes and (b) the Samail Ophiolite nappe, together with exotic blocks of distal origin (Glennie and others, 1974; Searle and Graham, 1982; Boudier and others, 1985; Béchennec, 1988; Beurrier and others, 1988; Hacker, 1994; Hacker and others, 1996; Pillevuit and others, 1997; Breton and others, 2004; Searle, 2007).

Three major structural units (e.g. Breton and others, 2004) form the Oman Mountains: Autochthonous, Allochthonous and Neo-Autochthonous. The first unit consists of an Autochthonous A, formed by a late Proterozoic crystalline basement (Roger and others, 1991) and a late Proterozoic to Devonian sedimentary sequence (Le Métour, 1988). These are unconformably overlain by Autochthonous B, which consists of a 2.5 km-thick middle Permian to late Cretaceous sedimentary sequence, made up of mostly shallow marine carbonates of the Arabian Platform. The Allochthonous is composed of the obducted and stacked Hawasina, Sumeini and Samail nappes, where the later is a relic of Cretaceous Neotethyan oceanic lithosphere (e.g. Beurrier, 1988). The Neo-Autochthonous unit overlies the other units above an unconformity and represents the post-obduction sedimentary cover of late Cretaceous to late Tertiary age (Glennie and others, 1974; Roger and others 1991; Breton and others, 2004; Fournier and others, 2006).

Several tectonic windows outcrop in the Oman Mountains below the ophiolites, but only two of them expose autochthonous rocks (fig. 1): the Jabal Akhdar window, which is the study

area of this contribution, and the Saih Hatat window. The degree of metamorphism is higher in the Saih Hatat area, which has blueschist and eclogite facies metamorphism, whereas there is a gradient of metamorphism from SW to NE in Jabal Akhdar, from upper anchizone up to pumpellyite/lawsonite facies (le Métour, 1988; Breton and others, 2004; Searle and others, 2004). Metamorphic peaks in the Saih Hatat window have been dated at ~80 Ma (Warren and others, 2003) and ~110 Ma (Gray and others, 2004a,b). The Jabal Akhdar is a 60 km wide flat top dome with flexure flanks parallel to the various directions of the borders.

A ~2500 m thick succession of Permian to Cenomanian carbonates is exposed in the core of the Jabal Akhdar dome (fig. 2; e.g. Glennie and others, 1974). We have focused this study on structures developed within Jurassic and Cretaceous limestones, clayey limestones and shales that are exposed along the southern, northern and eastern limbs of the Jabal Akhdar dome. These units are part of the Autochthonous B unit and belong to the Sahtan, Kahmah and Wasia groups of the Hajar Supergroup (Glennie and others, 1974; Beurrier and others, 1986; Glennie, 2005).

The sequence of Mesozoic carbonates of the Autochthonous B was deposited on the southern passive margin of the Tethyan Ocean during the breakup of Gondwana (Glennie and others, 1974; Hanna, 1990; Pratt & Smewing, 1993; Loosveld and others, 1996; Masse and others 1997, 1998; Hillgärtner and others, 2003; Breton and others, 2004; Glennie, 2005; Searle, 2007). According to Ziegler (2001) and Searle (2007) sedimentation was roughly continuous in the area.

The oldest rocks we have included in this study are Jurassic brownish shaley layers and blue limestones of the Awabi formation (Sahtan Group; fig. 2). A transition from a deepwater environment to an open-marine shelf and a shallow marine carbonate platform took place from the Tithonian (late Jurassic) to the end of the Cenomanian (Upper Cretaceous). During this time, the Kahmah and Wasia groups were deposited (fig. 2; Ziegler, 2001; Breton and others, 2004; Sharland and others, 2004). The Kahmah group consists of the Birkat and Shams formations. The first one is equivalent to the subsurface Salil formation (Hughes Clarke, 1988), and consists of clayey limestone and limestone. The Shams formation includes the subsurface Habshan, Lekhwair, Kharaib and Shu'aiba formations (Hughes Clarke, 1988) and contains thick-bedded

limestone. The Wasia group is formed by the Nahr Umr and the Natih formations. They consist of clayey limestone and thick-bedded limestone, respectively. The Mesozoic sequence formed by the Akhdar, Sahtan, Kahmah and Wasia groups was uplifted during the Early Turonian in response to the flexural bending of the foreland associated with the ongoing subduction, which was intra-oceanic according to Searle (2007) or intra-continental along the continental margin in the model by Breton and others (2004).

The last Autochthonous B unit is the Muti Formation (Aruma Group). It is composed of Turonian to Santonian wildflysch megabreccias and olistoliths. These sediments were deposited as a consequence of the transition from a passive continental margin to a foredeep basin (Breton and others 2004), and register a variation in sedimentary facies caused by migration of the depocenter towards the south due to the intra-margin subduction (Breton and others 2004) or intra-oceanic subduction (Searle, 2007). The Muti Fm was deposited during subduction, and obduction in the foredeep is stopped from North to South by the progressing overthrust. The Allochthonous unit is formed by the overthrusted Hawasina and Samail nappes (fig. 1). According to Glennie and others (1974), Nolan and others (1990) and Searle (2007) the nappe emplacement ended in the Early Campanian. The Campanian to early Tertiary limestones were deposited after the nappe emplacement (e.g. Glennie and others, 1973; Hanna, 1990).

The whole study area underwent later several episodes of extension and compression, uplift and doming. Filbrandt and others (2006) provided a synthesis of structural styles observed in the oil producing area Block 6, south of Jabal Akhdar. They identified strike-slip and normal faults formed under an overall NW-SE-oriented compression during the Campanian, associated to the oblique collision of the Indian and Arabian plates. Filbrandt and others (2006) interpreted that uplift and erosion during the Maastrichtian to Paleocene followed this faulting event. Finally, these authors propose a change of the stress field during the Late Cenozoic to NE-SW-oriented compression, which was probably associated to the uplift of the Oman Mountains. Fournier and others (2006) described structures formed in an extensional tectonic regime in the post-nappe units during the Late Cretaceous and early Cenozoic times. They found two undistinguishable extension directions (NNE-SSW and NW-SE) during the upper Eocene and Oligocene, followed by a compressional event (NE-SW to E-W-oriented compression) during

the late Oligocene (associated to the Arabia-Eurasia collision), and finally a recent N-S compression event during the Miocene-Pliocene. It is still debated whether uplift and doming took place during the Late Cretaceous (e.g. Bernoulli and others, 1990; Hanna, 1990), the Tertiary (e.g. Glennie and others, 1974) or during multi-phase deformation in the late Cretaceous to Early Paleocene and Miocene-Pliocene (e.g. Searle, 1985; 2007; Glennie, 1995; Poupeau and others, 1998; Gray and others, 2000).

PREVIOUS STUDIES OF VEINS, FAULTS AND FRACTURES IN JABAL AKHDAR

Filbrandt and others (2006) present a summary of structures found in Jabal Akhdar, and compare them to seismic-scale fault orientations found in Block 6 with seismic surveys. These authors pointed out that, due to the overburden of the Samail and Hawasina Nappes, the structures in Jabal Akhdar formed at a greater depth than those of Block 6. The outcropping structures described by Filbrandt and others (2006) include: (a) two sets of calcite-filled faults (striking 100-110º and 130-160º) related to the collision of Arabia with the India Plate during the Late Cretaceous; and (b) an additional set of NE-SW-striking open fractures formed during NE-SW-oriented compression and inversion during Miocene to recent collision of the Arabian plate with the Iran/Eurasia plates.

Hilgers and others (2006) proposed a total of 7 generations of veins and faults in the Jabal Akhdar dome. Their first generation of calcite veins formed in steeply inclined segments of stylolite seams (*V1*). These veins are crosscut by calcite veins perpendicular to bedding (*V2*), which are interpreted as extensional veins and strike N-S to NW-SE. A third generation of veins is described to occur in the form of pinch-and-swell structures, within cleaved marls (*V3*) and are interpreted to be consistent with a top-to-the-east shearing. *V3* is followed by the formation of bedding-parallel veins (*V4*) that truncate veins of set (*V2*) and show a top-to-NE layer-parallel shearing. The next vein event consists of veins associated with normal faults (*V5* and *V6*). *V5* veins are conjugate *en-échelon* arrays oriented perpendicular to bedding and strike parallel to normal faults (*V4*), while *V6* veins developed in dilatational jogs along the normal faults. Hilgers and others (2006) describe sub-vertical and sub-horizontal striations on the surfaces of the dilational jog veins. They interpret this strike-slip movement to have occurred after the normal

faulting. The last vein event (*V7*) described by Hilgers and others (2006) consists of veins developed within small WSW dipping thrusts and associated structures (folds and reverse folds). These are interpreted to result from the doming of Jabal Akhdar during the Tertiary (see Glennie and others, 1974; Gray and others, 2000). Based on stable isotope analysis, Hilgers and others (2006) argued that the fluids responsible for the formation of veins sets *V1* to *V5* were evolved meteoric waters or formation fluids buffered by host rocks. They associate the development of veins of sets *V6* and *V7* with more pristine fluids that had isotopically exchanged with silicates. According to them, this exchange probably took place during the drainage of the overpressured fluid, which led to a fluid pressure decrease at the time of normal faulting allowing the infiltration of meteoric fluids into the dome.

Holland and others (2009a; 2009b) studied the evolution of fractures and faults in the southern flank of the Jabal Akhdar dome. In the first of two publications Holland and others (2009a) summarize field observations of fracture and vein occurrence, together with descriptions of overprinting relationships, in several outcrops, including fluid inclusion microthermometry of some veins. The second contribution (Holland and others, 2009b) consists of a multiscale fracture and fault analysis based on satellite images. The authors concluded that there are four main vein/fracture/fault generations in the area: vein sets normal to bedding (*d1*), structures parallel to bedding (*d2*) including duplex structures indicating top to the South thrusting (*d**) and structures with shear indicators showing top- to the NE shear, (*d3*) normal faulting with throws up to 700 m, locally reactivated in strike-slip and (*d4*) uncemented or partly cemented joints and other recent structures. Holland and others (2009a; 2009b) did not discuss in detail the correspondence in relationships of their structural events with those of Hilgers and others (2006). In the study of Holland and others (2009a; 2009b) the definition of the first group of structures (bedding-normal veins, *d1*) was based on strike directions of veins and their relative overprinting relationships, and overprinting of bedding-normal veins by bedding-parallel shear. They found four strike classes (*d1*), and based on analysis of overprinting relationships, interpreted these as four generations of extensional veins with a progressive anti-clockwise rotation of the stress field. N-S striking veins were interpreted to have developed first, followed by NW-SE, E-W and, finally, NE-SW striking veins. A prominent process during the evolution of these veins was interpreted to have been repeated crack-seal cycles (Ramsay, 1980). Holland and Urai (2010)

presented a first attempt to relate the vein microstructure evolution to the strength contrast between vein and host rock.

Holland and others (2009a) obtained homogenization temperatures ranging from 84º and 130ºC and salinities from 3.8 to 6.0 eq. wt% NaCl measured from fluid inclusions, which were found in one of these bedding-parallel veins. After *d2*, normal faults of different scales (*d3*) were interpreted to have overprinted previous structures in response to a new stress field. Holland and others (2009a) associate *en-échelon* veins to this event and suggest that these structures were formed in a high-pressure environment. Finally, they describe recent structures, such as joints and uncemented or partly cemented fractures (*d4*) that strike into the directions of the first vein group perpendicular to the bedding (*d1*). These structures are interpreted as a result of exhumation and/or weathering.

The study of Holland and others (2009a; 2009b) was followed up by the work of Virgo and others (2013a), which confirmed the satellite-based data acquisition of faults, veins and joints of Holland and others (2009b) in a small area. The development of veins at high angle to bedding (*d1* of Holland and others (2009a)) was interpreted to extend to after the normal faulting (*d3* of Holland and others 2009a) and the timing of the normal faulting was interpreted to have started after the nappe emplacement and ended during the Campanian. In the interpretation of Holland and others (2009) and Virgo and others (2013a) the normal faults are of the same age as the regional normal- to oblique-slip faults in the subsurface of northern Oman and the United Arab Emirates, which evolved during the early deposition of the Fiqa Formation in the Campanian (Filbrandt and others 2006), and to be coeval with Phase I extension of Fournier and others (2006). According to Virgo and others (2013a), the reactivation of these faults and the evolution of new veins were followed by folding of the Jabal Akhdar dome and final uplift and jointing by reactivation of preexisting microveins.

METHODS OF ANALYSIS OF FRACTURES, VEINS AND STYLOLITES

Building on the studies reviewed above, we have collected over 600 three-dimensional measurements of fracture, fault and vein orientations, opening directions, striations on exposed

planes, stretched crystals and slickenfibres in veins, as well as stylolite orientations and roughness analysis. Overprinting relationships between the various structures (fig. 4) are used to constrain the tectonic evolution of the area. Our survey was performed in several outcrops in different areas of the Jabal Akhdar dome (fig. 3, table 1) located at the northern, eastern and southern limbs.

Veins were classified according to their geometry, internal structures (crystal growth direction, crystal morphology) and vein growth mechanism (Durney and Ramsay, 1973; Ramsay and Huber, 1983; Passchier and Trouw, 2005; Bons, 2001; Bons and others, 2012). The two main vein types we found are syntaxial and stretching or ataxial veins. Crystals in syntaxial veins grow towards the centre of the vein, where the vein opens. Opening can be one or several cracking events where the crack is located in the centre of the vein. Stretching (ataxial) veins are veins that form during crack-seal events where the location of the crack surface is randomly distributed through the vein. Transitions of one type to the other can be found in single veins (Bons and others, 2012). In the Oman Mountains many *en-échelon* vein arrays (Beach, 1975) can be found, where small parallel vein sets are offset relative to each other (fig. 4B). If these veins are curved they form sigmoidal sets. *En-échelon* vein sets are useful because they can be used as paleostress direction-indicators.

In the following section we describe the structures in the Oman Mountains by relative age. The orientation of the principal stress axes is determined using stress inversion methods (e.g. Ramsay and Lisle, 2000) (fig. 4A,B) and for cases where no fault-slip data are present, the principal axes of deformation were deduced from the geometric pattern of tectonic veins (e.g. Hancock, 1985). We have assumed that the principal stresses σ_1, σ_2 and σ_3 are parallel to the shortening, intermediate and extension axes, respectively.

RESULTS: SEQUENCE OF EVENTS AND PALEOSTRESS ORIENTATIONS

Event #1: Diagenetic Stylolites and Early Veins

The oldest structures after sedimentary bedding in Jabal Akhdar seem to be diagenetic stylolites and calcite veins with various orientations (Hilgers and others, 2006; fig. 7 of Holland and others, 2009). Two-dimensional spectral analysis of the roughness of these stylolites was used to estimate the paleodepth of their formation (see Ebner and others (2009) for details of the method). Five sedimentary stylolites were used for the analysis (fig. 5A), one from the Muti Fm, two from the Shams Fm (both Cretaceous), one from the uppermost part of the Awabi Fm (Jurassic) and one from the Saiq Fm (Permian). All these stylolites give a paleodepth estimate that is in accordance with their original stratigraphic depth. This suggests that the stylolites formed during the initial formation of the sequence before the nappes were thrusted on top of the sequence. Some of the highest diagenetic stylolites in the stratigraphic sequence tend to dissolve bedding-perpendicular veins. We interpret this as a reactivation of the stylolites due to the additional load that was applied on the sequence when the nappes were emplaced. Early veins are not frequent, do not show conjugate sets and so far show no consistent orientations, so that we cannot attribute them to a specific stress field. These bedding-confined veins are interpreted to be related to layer-normal compression due to burial (fig. 5B,C; Bons and others, 2012). Some of the early layer-perpendicular veins in Jabal Akhdar are crosscut by later veins that belong to a normal faulting event (event #3) and conjugate sets of strike-slip veins (events *#5* to *#7*).

Event #2: Top-to-the-South Layer-parallel Shearing

The second event that can clearly be distinguished is top-to-the-South shearing, as shown by layer-parallel veins with ca. N-S-oriented slickenfibres (fig. 6A,B,D). To our knowledge, these have not yet been reported in the literature. However, we found these at three different localities (numbers 1, 6 and 8 of table 1), where their slickenfibres show average azimuth orientations of 017º, 200º and 356º if we assume that layers were horizontal when the structures were developed (fig. 6C, table 2).

Event #3: Normal (dip-slip) Faults and Veins

Thrusting towards the south (event *#2*) is followed by the development of normal (i.e. dip-slip) to oblique-slip faults (event *#3*) (figs. 7, 8). Large-scale faults with a rough E-W strike

have stratigraphic offsets between meters and hundreds of meters (Holland and others, 2009a; Virgo and others, 2013a). Conjugate sets of normal faults show vertical or sub-vertical striations (fig. 7A,B, table 2). Normal faults are associated with sets of conjugate outcrop-scale faults and calcite *en-échelon* veins with an inferred sub-vertical principal compressive stress that can be identified in outcrops 1, 4, 5, 6, 7, 11 and 12 (tables 1, 2, figs. 7 A,B,E, 8). Sometimes only one fault set is present, although vertical striations indicate dip-slip movement (fig. 7C,D). Faults and veins can occasionally be oblique-slip and some 100 m to km-scale faults also show oblique-slip striations. In cases where multiple striation directions were observed on a single fault plane, the oblique-slip striations consistently overprint the dip-slip ones, and both are overprinted by later strike-slip striations (see sections below). Large-scale faults are offsetting structures related to event *#2* (top-to-the-South layer-parallel shearing; fig. 7F,H). Figure 7G shows the orientation of the average principal compressive stress for each outcrop calculated from normal faults and veins and illustrates that σ_1 was nearly vertical. The orientation of the stress field was calculated for each outcrop and then rotated back assuming that layers were horizontal at the time when the structures developed. If σ_1 and σ_2 are of similar magnitude, it is difficult to distinguish between an extensional and transtensional stress regime. But because overprinting striations consistently show a change from dip- and oblique-slip (event *#3*) towards strike-slip movement (see descriptions of events *#5* and *#6* below), we favor the interpretation that the stress regime was indeed extensional during event *#3* and later became transtensional to strike-slip. The interpretation of an extensional stress field is consistent with that of Hilgers and others (2006), Holland and others (2009a; 2009b) and Virgo and others (2013a). The damage zones of these faults are full of veins and carbonate breccias (fig. 8C-F) suggesting that they were at some stage preferential fluid pathways with high fluid pressures (Hilgers and others, 2006), probably during subsequent deformation events.

Event #4: Top-to-the-Northeast Layer-parallel Veins

Top-to-the-Northeast layer parallel shearing (event *#4*) can be clearly identified at localities 1, 3, 4, 5, 8 and 11 (tables 1, 2, fig. 9), and postdates structures of previous events. This regional event also produced ramps and duplexes that can be found in the northern flank of the dome (Breton and others, 2004; Hilgers and others, 2006; Al-Wardi and Butler, 2007). Calcite

372 and quartz slickenfibres and striations can be found on veins parallel to layers. In addition, veins
373 roughly parallel to cleavage planes are found in clayey beds (fig. 9A-C). Both structures show a
374 top-to-the-Northeast sense of shearing. The azimuth of these striations and the direction of
375 slickenfibres in veins vary on average between 025º and 072º when they plunge towards the
376 northeast and 231º when they plunge towards the southwest. These orientations have been
377 calculated considering that layers were horizontal when the structures were developed.
378 According to Breton and others (2004) and Al-Wardi and Butler (2007), cleavage in clayey
379 layers formed during this tectonic event. As the veins are roughly parallel to cleavage they
380 probably formed late, after the cleavage had rotated to an orientation favorable for the formation
381 of shear veins. The top-to-NE layer-parallel shearing is interpreted to be the result of tectonic
382 exhumation of the autochthonous as a consequence of a reversal of the movement that produced
383 the allochthonous emplacement (Miller and others; 1998). This tectonic event was extensively
384 reported by many studies, including le Métour (1988), Rabu (1988), Breton and others (2004 and
385 references therein), Al-Wardi and Butler (2006), Hilgers and others (2006), Searle (2007) and
386 Holland and others (2009a). These studies described structures produced by this event, including
387 layer-parallel shearing, formation of cleavage and nucleation of NE-directed ramps and
388 duplexes.
389
390 Small conjugate sets of normal faults filled with calcite are sheared parallel to layers
391 towards the NE in several outcrops of localities 4 and 5 (fig. 9A-C). The same overprint
392 relationship was also reported by Breton and others (2004). Some of the pre-existing veins are
393 passively sheared and form sigmoidal veins (fig. 9D). These relationships suggest that the top-to-
394 the-Northeast layer parallel shear is postdating a normal faulting event (*#3*), indicating that σ_1
395 rotated from layer-normal (vertical) towards North- to Northeast-plunging, which would have
396 resulted in a net layer-parallel shear stress. Existing faults probably remained active as long as
397 their orientation with respect to the stress field was favorable for it. Hilgers and others (2006)
398 and Holland and others (2009a) concluded that normal faulting also postdates NE layer parallel
399 shearing, because faults with dip-slip movements offsetting layer-parallel veins can also be
400 found throughout the area (figs. 3 and 4 of Hilgers and others, 2006). However, as explained in
401 the discussion section, it is not clear whether these structures formed by truly normal faulting or

by vertical block movement during subsequent strike-slip deformation events (see below), after the top-to-NE layer-parallel shearing.

Event #5: Strike-slip Faults, Tectonic Stylolites and Veins: NW-SE-oriented Compression

We find three distinct strike-slip events (σ_1 and σ_3 approximately horizontal) in the Jabal Akhdar area. The related structures include faults on different scales (from meters to kilometers), *en-échelon* conjugate sets of veins and tectonic stylolites that indicate a horizontal compression direction. The first strike-slip structures are *en-échelon* conjugate sets of veins formed during a NW-SE-oriented compression. These veins can be recognized at localities 8, 9 and 12, and are formed by many veins that crop out on polished surfaces or "pavements" (tables 1, 2, fig. 10). The vertical intersection of dextral and sinistral conjugate vein sets, together with the presence of sub-horizontal slickenfibres in veins (fig. 10A) show that these veins were formed as a consequence of a strike-slip stress field (fig. 10H). Tectonic stylolites that show a NW-SE oriented compression direction are also indicative of this strike slip event (fig. 11). Al-Wardi and Butler (2007) also found arrays of conjugate strike-slip faults accommodating NW-SE compression in Jebel Nakhl.

Some of the E-W striking large-scale normal faults (event *#3*) show sub-horizontal striations that postdate dip- or oblique-slip ones (e.g. fig. 10F). This indicates that the normal faults are reactivated during the strike slip events. In addition conjugate sets of *en-échelon* veins and new strike-slip faults formed. In many cases these sets of veins are strongly influenced by mechanical stratigraphy and rock texture, so that they are often restricted to certain layers, or they are continuous in one layer and segmented in the adjacent layer. Strike-slip deformation is postdating layer-parallel shearing as well as normal and oblique-slip faults and veins. On fault planes sub-horizontal striations are always postdating sub-vertical and oblique ones. *En-échelon* strike slip veins are crosscutting bedding parallel veins. Veins of strike-slip events (#5, #6, #7) typically have crack-seal microstructures, and were formed by hundreds to thousands of micro-cracking events (fig. 10G).

Event #6: Strike-slip Faults, Tectonic Stylolites and Veins: E-W-oriented Principal Compression

The initial group of strike-slip veins and faults (event *#5*) are clearly crosscut by a second group of strike-slip faults and *en-échelon* veins that formed under E-W-oriented compression (fig. 10B-E, I). A second set of tectonic stylolites also shows an E-W oriented compressive stress (fig. 11). This group of structures can be found in many outcrops across the Jabal Akhdar dome, including all the localities listed in tables 1 and 2, except for 4, 7 and 12. Veins that developed during event *#6* are similar to the event *#5* veins and are strongly influenced by the mechanical stratigraphy of the sequence. Some layer-parallel veins with top-to-the-East striations and slickenfibres can be found at locality 1. They seem contemporaneous with conjugate veins of event *#6* and, moreover, their displacement direction is compatible with E-W-oriented σ_1. We therefore suggest the possibility that local top-to-E slip also took place during event *#6*. Two events of strike-slip veins with σ_1 oriented approximately E-W, namely *#6a* and *#6b,* can be recognized at locality 1, with σ_1 oriented E-W and ESE-WNW, respectively (fig. 10B-E).

Event #7: Strike-slip Veins and Tectonic Stylolites: N-S to NE-SW-oriented Principal Compression

The last group of strike-slip veins was formed due to a N-S to NE-SW-oriented σ_1 (fig. 10J), and consist of conjugate sets of *en-échelon* veins, and can be identified at localities 1, 4 and 6 of tables 1 and 2. They cut veins of events *#5* and *#6* and their presence is considerably less intense than that of event *#6*. A small number of tectonic stylolites are associated with this tectonic event.

Event #8: Folding (Doming)

The uplift and folding of the Jabal Akhdar area (event *#8*) postdates the previously described events (*#1* to *#7*). Our data suggest that structures of all events *#1* to *#7* were tilted together with the sedimentary layers when Jabal Akhdar was folded.

The relative orientations and crosscutting relationships of structures of events *#1* to *#7*, measured at different outcrops through the Jabal Akhdar dome, coincide when data is rotated so

that layering is horizontal. All the presented stereograms up to event *#7* display rotated data. The doming could have reactivated old layer-parallel veins as well as some of the faults as normal or oblique-slip faults. However, we have not identified recent striations postdating strike-slip ones.

Hilgers and others (2006) mention late North-directed ramps in the Northern flank of the dome, and they leave open the possibility that these structures formed by flexural slip folding of the dome. Holland and others (2009a; 2009b) reported one South-directed ramp structure in Wadi Ghul, on the Southern flank of Jabal Akhdar (locality 13 in table 1). Bedding-confined veins (event *#1*) are rotated together with bedding in this ramp, implying that ramping postdates these veins. Holland and others (2009a) could not constrain the timing of this ramping in relation to other structures. The top-to-the-South movement on this ramp could have taken place either during event *#2* or during event *#8*.

Event #9: Joints

A final group of structures that can be recognized in the area are recent joints (fig. 12A,B) and very long and thin veins parallel to them (fig. 12C). These structures generally show no shear component and no displacements but are often parallel to thicker veins and could have been reactivated. The orientation of joints is constant across the whole area (fig. 12D). We measured joints in localities 1, 8 and 9 of tables 1 and 2 and found them to strike NNW-SSE and E-W. According to borehole breakouts from Block 6 (Filbrandt and others, 2006) the orientation of the present-day stress field corresponds to a NE-SW-oriented compression, with local variations to E-W or NW-SE. The last orientation is more compatible with the joint orientations in Jabal Akhdar.

DISCUSSION

Synthesis of Tectonic Episodes and Geodynamic Interpretation

On the basis of the presented field survey 9 structural events were recognized in Jabal Akhdar (table 3, fig. 13):

#1 - Diagenetic stylolites and early bedding-confined veins

#2 - Top-to-the-South layer-parallel shearing

#3 - Normal (dip-slip) faults and veins

#4 - Top-to-the-Northeast layer-parallel veins

#5 - Strike-slip veins, faults and tectonic stylolites: NW-SE-oriented compression

#6 - Strike-slip veins, faults and tectonic stylolites: E-W-oriented principal compression

#7 - Strike-slip veins and tectonic stylolites: N-S to NE-SW-oriented principal compression

#8 - Folding (doming)

#9 - Joints

The first event (*#1*) can be recognized by the presence of diagenetic stylolites and veins that appear in isolated sets, mostly perpendicular to layering. As mentioned earlier, a paleodepth analysis on some stylolites indicates that they formed during the initial compaction of the basin before the obduction of the Samail and Hawasina nappes. Holland and others (2009a) describe four families of bedding-normal veins with different strikes and suggest an anticlockwise rotation of the stress field (with vertical σ_1), before the onset of bedding-parallel shear. However, most of the layer-perpendicular veins described by Holland and others (2009a) are interpreted here as belonging to a later event. Hilgers and others (2006) found bedding-normal veins that formed after veins that can be found in inclined segments of stylolite seams. We interpret event *#1* veins in accordance with Hilgers and others (2006) as extensional veins that formed as a result of a vertical σ_1 that represents the overburden stress during basin subsidence. The existence of veins indicates that fluid pressures were probably supra-hydrostatic leading to a negative effective σ_3 in at least the more competent layers.

Bedding-normal veins of event *#1* are postdated by top-to-the-South layer-parallel veins with striations and slickenfibres (event *#2*). Breton and others (2004) interpret that at his time the top of the autochthonous was separated from the base of the nappes by the southern corner of the North Muscat microplate, which existed between the intra-continental and the intraoceanic subduction zones. Contrary to this, we interpret event *#2* as south-directed shearing of the

sequence that was induced by the obduction of the Samail ophiolite and Hawasina nappes during the Mid Turonian to Late Santonian.

Event *#3* records a large-scale extension of the area with normal faults and veins that are offset by a second bedding-parallel shearing event but with a top-to-NE movement (event *#4*). This event was also recorded by Breton and others (2004) and Hilgers and others (2006). Breton and others (2004) place the formation of the normal faults prior to the obduction event (*#2*), as a consequence of an extensional stress field associated to the intracontinental subduction (Cenomanian to Middle Turonian). However, these authors did not recognize the top-to-the-South layer-parallel shear veins. We found that faults with dip-slip striations offset veins of event *#2*, which implies that these faults postdate obduction. It should be noted, however, that normal faults can easily be reactivated as dip-, oblique- or strike-slip faults in later tectonic events. It is thus also possible that normal faults formed before event *#2*, as proposed by Breton and others (2004), and were later reactivated during strike-slip events (likely *#5* or *#6*) producing dip-slip movements and thus offsetting top-to-the-South layer-parallel veins (as in fig. 7F,H). Our field observations (fig. 9A,B), as well as those by Breton and others (2004) show that outcrop-scale normal faults are clearly sheared by the top to the NE movement, contrary to Holland and others (2009a; 2009b), who place the onset of normal faults after top-to-the-NE shear. Hilgers and others (2006) suggest that normal faults occur both before and after top-to-NE shearing. Fault reactivation during strike-slip events (namely *#5*, *#6* and *#7*) causing vertical block movements with a dip-slip component can explain the apparent normal faulting after event *#4*. A second, truly normal faulting event (i.e. with vertical σ_1) is thus uncertain, but cannot be excluded. Hilgers and others (2006) propose fluid pressures close to lithostatic for these phases.

The formation of regional-scale cleavage across Jabal Akhdar during N- to NE- directed shearing has been extensively described by many authors, including le Métour (1988), Rabu and others (1993), Breton and others (2004), Al-Wardi (2006), Al-Wardi and Butler (2006) and Searle (2007), together with structures such as shear bands, rotation of pinch-and-swell veins, striations and offsets on layer-parallel veins indicating this sense of movement. Our observations confirm that veins indicating top-to-NE shearing also occur subparallel to cleavage in clayey layers (especially in Wadi Nakhar). We thus think that they were formed during event *#4*, but

after cleavage was already formed and rotated to a favorable orientation for opening. According to Breton and others (2004) exhumation of the autochthonous and back- (i.e. reverse-) top-to-NE shearing took place during the Early Campanian to Early Maastrichtian.

Late in or after the exhumation stage the study area was subjected to several strike-slip events. We found three distinct events with a horizontal compressive stress that belong to strike slip events: *#5* (NW-SE-oriented σ_1), *#6* (E-W-oriented σ_1) and *#7* (N-S to NE-SW-oriented σ_1). The associated structures consist of conjugate arrays of *en-échelon* crack-seal calcite veins, tectonic stylolites as well as both new and reactivated faults. Many of the outcrops containing the highest vein density are located at the top of the Natih Fm, just below the contact between the Natih and the Muti Fms (table 1). The studies of Hilgers and others (2006) and Holland and others (2009a) briefly mention a transition of dip-slip to strike-slip deformation of normal faults (*#3*), but they did not recognize the abundant conjugate calcite vein sets that belong to the three strike slip events (*#5*, *#6* and *#7*) and the ubiquitous horizontal or subhorizontal striations on large-scale fault planes (fig. 11B). Therefore, these studies underestimated the importance of the strike-slip events, which could have also reactivated older faults (event *#3*) with offsets that have a vertical component, as discussed above. Al-Wardi and Butler (2007) described conjugate strike-slip faults formed under NW-SE-directed compression in Jabal Nakhl, and they suggested that they formed during the formation (folding) of this antiform.

Due to the lack of a Tertiary cover in the Jabal Akhdar dome, it is difficult to know the exact age of strike-slip structures. Strike-slip deformation with the same orientation as our event *#5* and *#6* has been extensively described in Early Cretaceous rocks of Oman. This deformation event formed the traps for the oil fields of Block 6 (Filbrandt and others, 2006) as well as in Abu Dhabi (Johnson and others, 2005). Moreover, a tectonic survey in Tertiary rocks (Fournier and others, 2006) also led to the conclusion that horizontal σ_1-σ_3 is responsible for the origin of Oligocene to Early Miocene strike slip structures.

Large-scale faults with both horizontal and vertical displacements are recognized from seismic surveys in Cretaceous rocks of the oil-producing Block 6. Filbrandt and others (2006) found that these structures were formed as a consequence of NW-SE-directed horizontal

588 compression (125 to 135º SW). They indicate that strike-slip deformation is prevalent in the
589 North of Block 6, and that the vast majority of faults are segmented. This is a typical feature of
590 structures with dominating strike-slip components (e.g. Richard and others, 1995). Moreover, the
591 density of these large-scale segmented faults decreases both downwards and upwards from the
592 top of the Natih Fm. As mentioned above, this also applies to the small-scale structures we have
593 described in the present study. Three major fault orientations are defined by Filbrandt and others,
594 (2006) at Block 6: (1) E-W to ESE-WNW-oriented *en-échelon* left-stepping arrays with dextral
595 strike-slip displacement, (b) NNW-SSE to N-S-oriented *en-échelon* right-stepping arrays with
596 sinistral strike-slip displacement and (c) faults oriented NW-SE. They attribute these structures
597 to a NW-SE-oriented compression during the Santonian to Campanian. According to them, this
598 stress field orientation would have persisted until the Early Miocene, when compression rotated
599 towards NE-SW. We propose that the structures of event *#5* of our study could have been formed
600 at the same time as those found at Block 6. This can be supported by the coincidence of stress
601 field orientation, structural style (segmented *en-échelon* arrays) and the maximum fracture
602 density at the top of the Natih Fm. Filbrandt and others (2006) attribute the origin of the NW-SE-
603 oriented maximum compression to the oblique collision of the Indian Plate against the Arabian
604 Plate during the Santonian to Campanian, although they specifically propose a Campanian age
605 for these faults. The overprint of tectonic structures in Jabal Akhdar suggests that strike-slip
606 deformation of event *#5* should have taken place after the top-to-NE layer-parallel shearing. This
607 restricts the aforementioned time span, so that strike-slip deformation in Jabal Akhdar could have
608 only started in the Mid Campanian. The horizontal σ_1 could have lasted at least until the
609 Maastrichtian, as this is the time of oblique transpression between the Arabian and Indian Plates.
610
611 Structures of event *#5* in Jabal Akhdar are clearly crosscut by ubiquitous arrays of *en-*
612 *échelon* calcite veins of event *#6*. These structures were formed due to an E-W-oriented
613 horizontal σ_1. Event *#6* is responsible for most of the fracture density and intensity in the studied
614 outcrops, and structures of this event are found in almost all the studied outcrops (table 2). As in
615 the case of event *#5*, fracture density of *#6* structures decreases both downwards and upwards
616 from the top of the Natih Fm. Large-scale faults with both horizontal and vertical displacements
617 have been described from seismic surveys in Cretaceous rocks in oil fields onshore and offshore
618 Abu Dhabi (e.g. Marzouk and Sattar, 1995; Johnson and others, 2005). These structures appear

to be contemporaneous with the segmented faults of Block 6 in Oman (Filbrandt and others, 2006), but they were formed due to E-W-oriented maximum horizontal compression (Marzouk and Sattar, 1995; Johnson and others, 2005). In the studied outcrops of Jabal Akhdar, *#6* structures are always crosscutting *#5* structures, so that at some stage the stress field changed from NW-SE to E-W horizontal compression. Structures of events *#5* and *#6* have many similarities in vein microstructures, fracture/vein segmentation, statistical distribution and mineral infillings (Stark, 2011), as well as conjugate angles between sets (see next section). These observations could indicate that they were formed without a major time span between one and the other. The coincidence of structural styles and orientations with Abu Dhabi segmented faults could suggest that *#6* structures in Jabal Akhdar could have also formed from the Mid Santonian to Maastrichtian. However, Breton (pers. com.) indicates that the area between Jabal Akhdar and Abu Dhabi is only affected by a major tectonic phase during the Aquitanian to the Late Langhian (Miocene). Moreover, Filbrandt and others (2006) and Breton (pers. com.) propose that the stress field orientation of event *#5* lasted until the Early Miocene, thus implying that structures of event *#6* were formed later than that. Fournier and others (2006) analyzed structures in Late Cretaceous and Cenozoic post-nappe (i.e. Neo-Autochthonous) units. They identified two extension directions during the upper Eocene and Oligocene, with extension oriented N20ºE and N150ºE, respectively. We have not recognized such events in the outcrops we have studied in Jabal Akhdar. Fournier and others (2006) also report E-W- to NE-SW-oriented compression during the Early Miocene, mainly documented by numerous conjugate strike-slip and reverse faults in the post-nappe units. These authors suggest that this compression phase could have started earlier in Jabal Akhdar, during the late Oligocene, since this area was uplifted between 30 and 25 Ma (Mount and others, 1998). The structures of our event *#6* could have very likely formed at this stage, as suggested by their coincidence with those in the Neo-Autochthonous units.

The low acute angles between conjugate sets (see next section) of structures of events *#5* and *#6*, especially in the Natih Fm, indicate a relatively high angle of internal friction that can be related to high fluid pressures. Such fluid pressures, also recognizable by the ubiquitous crack-seal microstructures of the veins of these events, can easily arise during exhumation (Staude and others, 2009). Fluid pressure in the crust typically increases from hydrostatic close to the surface

to lithostatic at depth. When the overburden pressure is reduced (i.e. decompression takes place), pore fluid pressure does not initially change, as the volume of pores remains approximately the same. Such a scenario can lead to the pore fluid pressure exceeding the host rock pressure, thus enhancing the formation of fractures through which fluids can escape (Staude and others, 2009; Weisheit and others, 2013). The overburden pressure can be reduced by erosion, thinning of the crust or crustal extension. According to Breton and others (2004) the burial conditions of the authochthonous remained approximately constant from the end of the Cretaceous until the Early Miocene. During that time, the removal of material due to the partial erosion of the ophiolites was compensated by the deposition of the Tertiary Marine sequence. As mentioned above, the Jabal Akhdar area experienced a general uplift during the Late Oligocene to the Early Miocene, which is the time when veins of event *#6* probably formed. Uplift can explain the high fluid pressure characteristics of this vein network, as well as their stratigraphic position, as event *#6* vein density and intensity are maximum at the top of the Natih Fm, just below the Muti Fm, which could have acted as a seal. Veins of events *#6* and *#7* are strongly influenced by mechanical stratigraphy, in a way that the sedimentary facies and the diagenetic features of the different layers determine whether the veins are restricted to certain layers, or whether they are continuous or segmented. However, the impact of mechanical stratigraphy on vein geometries is beyond the scope of this study. Richard and others (2014) provide a discussion of the segmentation nature of faults of different scales and the influence of mechanical lithologies in North Oman.

The third strike slip event (*#7*) formed during N-S to NE-SW-oriented horizontal compression. The exact age of these structures is not clear, but they probably formed during the Late Miocene to the Pliocene. Apart from a small number of late Paleocene faults with NNE-SSE-oriented σ_1 identified in the North part of Block 6 (Filbrandt and others, 2006), numerous structures formed under N-S- to NNE-SSW-directed compression in post-nappe units during the Pliocene (Fournier and others, 2006).

All the aforementioned structures (*#1* to *#7*) are tilted together with sedimentary layers during doming of Jabal Akhdar in the Pliocene. When layers are rotated back to horizontal in the northern, southern and eastern flanks of the Jabal Akhdar dome, structure orientations and timing

are consistent. The late development of the current dome has been extensively described in the literature (e.g. Carbon, 1996; Poupeau and others, 1998). The vertical uplift of the area during the Pliocene-Quaternary could have reactivated some of the faults (Hanna, 1986; Patton and O'Connor, 1988; Mann and others, 1990; Carbon, 1996; Poupeau and others, 1998; Hilgers and others, 2006), although we could not identify dip-slip striations postdating strike-slip ones. Small thrusts, associated folds and reverse faults associated to compression are reported at the northern flank of the dome (Hilgers and others, 2006). These authors suggest that these structures formed during the doming of Jabal Akhdar. It is possible that event *#7* (N-S compression) occurred during the early stages of event *#8* (doming). Finally, joints are the most recent structures in the area (*#9*). They may have formed by decompression during exhumation or as a consequence of the present-day stress field in NE Oman.

There are many examples in the literature of case studies where fracture or joint formation and reactivation are strongly influenced by the development of one or several folds (e.g. Engelder and Peacock, 2001; DiNaccio and others, 2005; Cassini and others, 2011; Tavani and others, 2011; Reif and others, 2012). However, it is important to remark here that, because the dome formation is a late event, the vast majority of the structures found in Jabal Akhdar are not related or influenced by it.

The main events in the area belong to four principal tectonic stages (see stereogram in fig. 13): (i) subduction, obduction and collapse of the nappe stack, (ii) reverse shearing and exhumation, (iii) far-field stress-driven strike slip deformation, and finally (iv) doming. First the top-to-S obduction of the Hawasina and Samail ophiolite nappes (*#2*) was probably followed by normal faulting due to gravitational loading (*#3*). Top-to-NE reverse shearing due to exhumation (*#4*) took place after that. These stages are overprinted by structures that developed as a consequence of a far-field horizontal compression stress field associated with the interaction between the Indian and Arabian plates, leading to three different tectonic phases (events *#5* to *#7*). All of the events can be observed and recorded in small-scale vein arrays and stylolites as well as in associated fault sets. Doming (*#8*) and, finally, joint formation (*#9*) were the latest events.

Use of Fractures/Veins as Indicators of Effective Fluid-Pressure Distribution

Most of the vein arrays in the Oman Mountains are conjugate sets of either continuous or *en-échelon* veins. If we assume a Mohr-Griffith-Coulomb failure criterion, the acute angle between conjugate sets (α) of structures of the same event can be used as a proxy for the relative differences in fluid pressure between different stratigraphic levels (Secor, 1965; Engelder, 1987; Bons and others, 2012). If we assume that the principal compression stress σ_1 lies on the acute bisector between two conjugate sets of veins or fractures, we can easily find the angle ζ between each set and σ_1:

$$\zeta = 45 - \phi / 2 \quad (1)$$

where ϕ is the angle of internal friction ($0^\circ \leq \phi \leq 90^\circ$). In a Mohr diagram the fluid pressure (P_f) shifts the Mohr circle towards the left (σ_n - σ_s) (fig. 14), so that a higher effective fluid pressure causes an increase of ϕ and a decrease of ζ.

If ϕ is 90º (fig. 14b) extensional fractures are formed (parallel to σ_1), and only one vein set forms. In this case there is a significant opening component in the fracture, but no shearing. If ϕ is relatively high (fig. 14c) we can expect the onset of hybrid fractures, with both shear and opening components. If ϕ is relatively low (fig. 14d) two conjugate sets of shear fractures may develop. If these sets are segmented, as is the case for most of the vein arrays described in this contribution, then conjugate sets of *en-échelon* veins may develop, as the individual fracture segments form at a low angle with respect to σ_1, and a significant opening component facilitates mineral precipitation. In conclusion, the angle between two conjugate sets of veins should be inversely proportional to the difference between lithostatic pressure and fluid pressure.

Holland and others (2009a) and Holland and Urai (2010) proposed the existence of a high-pressure cell prior and during the normal faulting event based on stable isotope data by Hilgers and others (2006) and fluid inclusion microthermometry by Holland and others (2009a). Within a single high-pressure cell, pore fluid is assumed to be connected and fluid pressure thus increases with depth by about 10 MPa/km. As a consequence, the difference between lithostatic

743 and hydrostatic pressure and, hence, the conjugate angle ζ should increase with depth. This angle
744 is plotted as a function of depth in figure 15. Contrary to Holland and others (2009a) and Holland
745 and Urai (2010), we only find indications for the existence of a high-pressure cell that spans the
746 entire sequence during events *#5* and *#6* (strike-slip deformation with NW-SE and E-W-oriented
747 σ_1, respectively). This is consistent with the observation of highest vein density in the Natih Fm,
748 which makes the Muti Fm the inferred seal.
749
750 The high-pressure cell would thus have formed at some stage between the Mid
751 Campanian to the Late Oligocene or Early Miocene. It is very likely that high fluid pressures
752 arose during the latter time span, when the area experienced significant exhumation and erosion.
753 Decompression probably released the fluids (Staude and others, 2009; Weisheit and others,
754 2013) and produced the fracture connectivity to build the tall high-pressure cell. It should,
755 however, be borne in mind that fluid pressure may not be the only factor that controls the angle
756 between conjugate sets of veins, the relative weight of shear and opening components, or the
757 degree of segmentation. Other factors that may potentially influence these are: rock texture
758 (grain size distribution, grain types, percentage of matrix and cements, etc.), rock cohesion,
759 presence of stylolites or pre-existing structures, layer thickness, lithologies above and below and
760 variable stress fields.
761
762 It is interesting to note that faults and fractures in the Jabal Akhdar dome seem to seal and
763 reopen repeatedly. Even small single veins show multiple crack-seal events. This behavior of
764 fracturing and resealing seems to happen on various scales in space and time. Hilgers and others
765 (2006) could show that fluid pressures were building up after the ophiolite was obducted. In their
766 model, these pressures remained high for part of the normal-faulting episode but then the high-
767 pressure cell opened and leaked through the faults. Here we could show that, if that ever
768 happened, the Jabal Akhdar resealed again, and that the fluid pressure was high during the strike-
769 slip events. Single local veins seem to show numerous crack-seal increments illustrating that the
770 small system opens and reseals on small time scales. In contrast, it seems that the larger systems
771 on the scale of the whole Jabal Akhdar dome open and reseal on much longer time scales.
772
773 **CONCLUSIONS**

This study uses fracture, vein, fault and stylolite data sets in order to reconstruct the complex and very dynamic deformation history of the Mesozoic autochthonous succession of the Jabal Akhdar dome, in the Oman Mountains. We determine the paleostress orientation history of the succession and correlate the results with the main tectonic events in the Northeast Arabian plate during the Late Cretaceous and Tertiary.

The oldest structures in the Mesozoic rocks after sediment deposition consist of early unsystematic veins and diagenetic (i.e. layer-parallel) stylolites formed during subsidence and subduction after subsidence. Subsequent structures can be assigned to the following main tectonic events that affected the area:

(1) Obduction of the Samail Ophiolite and Hawasina nappes. Layer-parallel veins with top-to-the-South striations and slickenfibres register the movement of the layers during this movement. Probably after that, seismic- and subseismic-scale normal (dip-slip) to oblique-slip faults and veins were formed as a consequence of crustal loading due to the nappe stack.

(2) Top-to-NE layer-parallel shearing associated to exhumation produced striations and slickenfibres in layer-parallel veins, as well as cleavage in clayey and marly layers.

(3) Oblique transpression between the Arabia and Indian plates in a time span between the end of the Cretaceous and the Miocene. The aforementioned structures are crosscut by three distinct strike-slip events. Structures mainly consist of conjugate sets of *en-échelon* calcite veins that form complex networks, as well as the reactivation of pre-existing faults of different scales and the onset of new ones. These structures were formed as a consequence of horizontal principal compression in three phases: NW-SE, E-W and, finally, N-S to NE-SW. The orientations and style of structures of the two first strike-slip events are compatible with those observed in seismic profiles in the neighboring hydrocarbon reservoirs of Oman and Abu Dhabi. The first one is probably coetaneous with these structures, while the second one is probably younger.

(4) Doming and formation of associated small thrusts, folds and reverse faults. The last strike-slip event could be coetaneous with doming.

A high-pressure cell, as proposed by Holland and others (2009a) and Holland and Urai (2010), could have existed in the area from the obduction of the Samail and Hawasina nappes until the Miocene. Most of the veins and fractures of different scales in Jabal Akhdar seem to have repeatedly opened and sealed, indicating an unstable dynamic system with relatively high fluid pressures. Moreover, the increasing vein/fracture intensity towards the top of the Natih formation, as well as the small angle between conjugate sets of veins of the NW-SE and E-W-oriented compression strike-slip events support the existence of high fluid pressures during the Late Cretaceous to Miocene. However, the highest overpressure and thus repeated crack-sealing probably took place during the Late Oligocene to Miocene.

This study shows how a detailed study of small-scale structures, readily visible in outcrop, can provide evidence for the succession of events on a much larger scale. This is of relevance to hydrocarbon exploration where only seismic-scale structures can be observed, but also to gain insight in plate tectonic movements, such as the convergence of Arabia and Eurasia and the relative movements of the Arabian and Indian plates.

ACKNOWLEDGEMENTS

This study was carried out within the framework of DGMK (German Society for Petroleum and Coal Science and Technology) research project 718 "Mineral Vein Dynamics Modelling", which is funded by the companies ExxonMobil Production Deutschland GmbH, GDF SUEZ E&P Deutschland GmbH, RWE Dea AG and Wintershall Holding GmbH, within the basic research program of the WEG Wirtschaftsverband Erdöl- und Erdgasgewinnung e.V. We thank the companies for their financial support and their permission to publish these results. The German University of Technology in Oman (GU-Tech) is acknowledged for its logistic support. We gratefully acknowledge the reviewers Andrea Billi and Jean-Paul Breton, whose constructive reviews greatly improved the manuscript, together with the editorial guidance of Danny M. Rye.

REFERENCES

836
837 Al-Wardi, M., 2006, Structural evolution of the Jebel Akhdar culmination and its implications
838 for exhumation processes in the northern Oman Mountains: Ph.D. thesis, University of
839 Leeds, UK.
840 Al-Wardi, M., and Butler, R. W. H. , 2006, Constrictional extensional tectonics in the northern
841 Oman Mountains, its role in culmination development and the exhumation of the
842 subducted Arabian margin, *in* Ries, A. C., Butler, R. W. H. and Graham, R. H., editors,
843 Deformation of the Continental Crust: The Legacy of Mike Coward. Geological Society
844 of London Special publication, v. 272, p. 187-202.
845 Beach, A., 1975, The geometry of en-echelon vein arrays: Tectonophysics, v. 28, p. 245-263.
846 Bechennec, F., le Metour, J., Rabu, D., Villey, M., and Beurrier, M., 1988, The Hawasina basin:
847 a fragment of a starved passive continental margin, thrust over the Arabian platform
848 during obduction of the Sumail nappe: Tectonophysics, v. 151, p. 323-343.
849 Bernoulli, D., Weissert, H., and Blome, C. D., 1990, Evolution of the Triassic Hawasina Basin,
850 Central Oman Mountains, *in* Robertson, A. H. F., Searle, M. P., and Ries, A. C., editors,
851 The Geology and Tectonics of the Oman Region: Geological Society of London Special
852 Publication, v. 49, p. 189-202.
853 Beurrier, M., 1988, Géologie de la Nappe Ophiolitique de Samail dans les Parties Orientale et
854 Centrale des Montagnes d'Oman: Ph.D. thesis, Pierre et Marie Curie University, Paris 6,
855 France.
856 Beurrier, M., Bechennec, F., Hutin, G., and Rabu, D., 1986, Rustaq, Geological Map Oman,
857 Scale 1:100,000, Sheet NF40-3D, Ministry of Petroleum and Minerals, Sultanate of
858 Oman.
859 Bons, P.D., Elburg, M.A., and Gomez-Rivas, E., 2012, A review of the formation of tectonic
860 veins and their microstructures: Journal of Structural Geology, v. 43, p. 33-62.
861 Boote, D. R. D., Mou, D., and Waite, R. I., 1990, Structural evolution of the Suneinah Foreland,
862 Central Oman Mountains, *in* Robertson, A. H. F., Searle, M. P., and Ries, A.C., editors,
863 The Geology and Tectonics of the Oman Region: Geological Society of London Special
864 Publication, v. 49, p. 397-418.

865 Boudier, F., Bouchez, J. L., Nicolas, A., Cannat, M., Ceuleneer, G., Misseri, M., and Montigny,
866 R., 1985, Kinematic of oceanic thrusting in the Oman Ophiolite: model for plate
867 convergence: Earth and Planetary Science Letters, v. 75, p. 215-222.
868 Breton, J. P., Bechennec, F., le Metour, J., Moen-Maurel, L., and Razin, P., 2004, Eoalpine
869 (Cretaceous) evolution of the Oman Tethyan continental marin: Insights from a structural
870 field study in Jabal Akdhar (Oman mountains): GeoArabia, v. 9, p. 1-18.
871 Casini, G., Gillespie, P. A., Verges, J., Romaire, I., Fernandez, N., Casciello, E., Saura, E., Mehl,
872 C., Homke, S., Embry, J.-C., Aghajari, L., and Hunt, D.W., 2011, Sub-seismic fractures
873 in foreland fold and thrust belts: insight from the Lurestan Province, Zagros Mountains,
874 Iran: Petroleum Geoscience, v. 17, p. 263-282.
875 Carbon, D., 1996, Tectonique post-obduction des montagnes d'Oman dans le cadre de la
876 convergence Arabie-Iran: Ph.D. thesis, Universite Montpellier II, France.
877 Cox, S.F., Braun, J., Knackstedt, M.A., 2001, Principles of structural control on permeability and
878 fluid flow in hydrothermal systems: Reviews in Economic Geology, v. 14, p. 1-24.
879 Durney, D.W., and Ramsay, J.G., 1973, Incremental strains measured by syntectonic crystal
880 growths, *in* De Jong, K.A., and Scholten, K., editors, Gravity and Tectonics: Wiley, New
881 York, p. 67-96.
882 Ebner, M., Koehn, Daniel , Toussaint, R., Renard, F. and Schmittbuhl, J., 2009, Stress
883 sensitivity of stylolite morphology. Earth and Planetary Science Letters, v. 277, p. 394-
884 398.
885 Ebner, M., Toussaint, R., Schmittbuhl, J., Koehn, D., and Bons, P.D., 2010, Anisotropic scaling
886 of tectonic stylolites: a fossilized signature of the stress field?: Journal of Geophysical
887 Research, v. 115, B06403, doi:10.1029/2009JB006649.
888 Engelder, T., 1987, Joints and shear fractures in rock, *in* Atkinson, B.K., editor, Fracture
889 Mechanics of Rock: Academic Press, London, p. 27-69.
890 Engelder, T., and Peacock, D.C.P., 2001, Joint development normal to regional compression
891 during flexural-flow folding: the Lilstock Buttress anticline, Somerset, England: Journal
892 of Structural Geology, v. 23, p. 259-277.
893 Etheridge, M.A., 1983, Differential stress magnitudes during regional deformation and
894 metamorphism: upper bound imposed by tensile fracturing: Geology, v. 11, p. 231-234.

895 Filbrandt, J. B., Al-Dhahab, S., Al-Habsy, A., Harris, K., Keating, J. , Al-Mahruqi, S., Ozkaya,
896 S. I., Richard, P. D., and Robertson, T., 2006, Kinematic interpretation and structural
897 evolution of North Oman, Block 6, since the late Cretaceous and implications for timing
898 of hydrocarbon migration into Cretaceous reservoirs: GeoArabia, v. 11, p. 97-140.
899 Fournier, M., Lepvrier, C., Razin, P., and Jolivet, L., 2006, Late Cretaceous to Paleogene post-
900 obduction extension and subsequent Neogene compression in the Oman Mountains:
901 GeoArabia, v. 4, p. 17-40.
902 Glennie, K. W., Boeuf, M. G. A., Hughes Clarke, M. W., Moody-Stuart, M., Pilaar, W. F. H.,
903 and Reinhardt, B. M., 1973, Late Cretaceous nappes in Oman mountains and their
904 geological evolution: AAPG Bulletin, v. 75, p. 5-27.
905 Glennie, K. W., Boeuf, M. G. A., Hughes-Clarke, M. W., Moody-Stuart, M., Pilaar, W. F. H.,
906 and Reinhardt, B. M., 1974, Geology of the Oman Mountains (Parts 1, 2 and 3):
907 Verhandelingen Koninklijk Nederlands Geologie en Mijnbouw Genootschap, v. 31, The
908 Hague, Martinus Nijhoff.
909 Glennie, K. W., 1995, The Geology of the Oman Mountains.
910 Glennie, K. W., 2005, The Geology of the Oman Mountains - An outline of their origin:
911 Scientific Press Ltd.
912 Gray, D. R., Gregory, R. T., and Miller, J. M., 2000, A new structural profile along the Muscat-
913 Ibra transect, Oman: Implications for emplacement of the Samail ophiolite, *in* Dilek, Y.,
914 Moores, E. M., Elthon, D., and Nicolas, A., editors, Ophiolites and Oceanic Crust: New
915 Insights from Field Studies and the Ocean Drilling Program, Geological Society of
916 America Special Paper. Geological Society of America, p. 513-523.
917 Gray, D. R., Hand, M., Mawby, J., Armstrong, R. A., Miller, J. M., and Gregory, R. T., 2004a,
918 Sm-Nd and Zircon U-Pb ages from the garnet bearing eclogites, NE Oman: Constraints
919 on High-P metamorphism: Earth and Planetary Science Letters, v. 222, p. 407-422.
920 Gray, D. R., Miller, J. M., Foster, D. A., and Gregory, R. T., 2004b, Transition from subduction-
921 to exhumation-related fabrics in glaucophanebearing eclogites, Oman: evidence from
922 relative fabric chronology and 40Ar/39Ar ages: Tectonophysics, v. 389, p. 35-64.
923 Hacker, B. R., 1994, Rapid emplacement of young oceanic lithosphere: argon geochronology of
924 the Oman ophiolite: Science, v. 265, p. 1536-1565.

925 Hacker, B. R., Mosenfelder, J. L., and Gnos, E., 1996, Rapid emplacement of the Oman
926 ophiolite: thermal and geochronological constraints: Tectonics, v. 15, p. 1230-1247.
927 Hancock, P. L., 1985, Brittle microtectonics: principles and practice: Journal of Structural
928 Geology, v. 7, p. 437-457.
929 Hanna, S.S., 1986, The Alpine (Late Cretaceous and Tertiary) tectonic evolution of the Oman
930 Mountains: a thrust tectonic approach. In: Symposium on the Hydrocarbon Potential of
931 Intense Thrust Zone. OAPEC, Kuwait, 2, p. 125-174.
932 Hanna, S. S., 1990, The Alpine deformation of the central Oman Mountains, *in* Robertson, A. H.
933 F., Searle, M. P., and Ries, A. C., editors, The Geology and Tectonics of the Oman
934 Region: Geological Society of London Special Publication, v. 49, p. 341-359.
935 Hilgers, C., Kirschner, D. L., Breton, J.-P., and Urai, J. L., 2006, Fracture sealing and fluid
936 overpressures in limestones of the Jabal Akhdar dome, Oman mountains. Geofluids, v. 6,
937 p. 169-184.
938 Hillgärtner, H., van Buchem, F. S. P., Gaumet, F., Razin, P., Pittet, B., Grötsch, J., and Droste,
939 H., 2003, The Barremian-Aptian evolution of the eastern Arabian carboante platform
940 margin (northern Oman): Journal of Sedimentary Research, v. 73, p. 756-773.
941 Holland, M., Urai, J. L., Muchez, P., and Willemse, E. J. M., 2009a, Evolution of fractures in a
942 highly dynamic, thermal, hydraulic, and mechanical system - (I) Field observations in
943 Mesozoic Carbonates, Jabal Shams, Oman Mountains: GeoArabia, v. 14, p. 57-110.
944 Holland, M., Saxena, N., and Urai, J.L., 2009b, Evolution of fractures in a highly dynamic
945 thermal, hydraulic, and mechanical system - (II) Remote sensing fracture analysis, Jabal
946 Shams, Oman Mountains: GeoArabia, v. 14, p. 163-194.
947 Holland, M., Urai, J.L., 2010, Evolution of anastomosing crack-seal vein networks in limestones:
948 insight from an exhumed high pressure cell, Jabal Shams, Oman Mountains: Journal of
949 Structural Geology, v. 32, p. 1279-1290.
950 Hubbert, M.K., and Rubey, W.W., 1959, Role of fluid pressure in mechanics of overthrust
951 faulting: Bulletin of the Geological Society of America, v. 70, p. 115-166.
952 Hughes Clarke, M. W., 1988, Stratigraphy and rock unit nomenclature in the oil-producing area
953 of interior Oman: Journal of Petroleum Geology, v. 11, p. 5-60.
954 Jaeger, J.C., Cook, N.G.W., and Zimmerman, R., 2007, Fundamentals of Rock Mechanics. 4th
955 Edition: Wiley-Blackweel, 488 pp.

956 Johnson, C. A., Hauge, T., Al-Menhali, S., Bin Sumaidaa, S., Sabin, B., and West, B., 2005,
957 Structural Styles & Tectonic Evolution of Onshore & Offshore Abu Dhabi, UAE,
958 International Petroleum Technology Conference (IPTC), Doha-Qatar.
959 Koehn, D., Toussaint, R.F., and Passchier, C.W., 2007, Growth of stylolite teeth pattern
960 depending on normal stress and finite compaction: Earth and Planetary Science Letters, v.
961 257, p. 582-595.
962 Koehn, D., Ebner, M., Renard, F., Toussaint, R., and Passchier., C.W., 2012, Modelling of
963 stylolite geometries and stress scaling: Earth and Planetary Science Letters, v. 341-344, p.
964 104-113.
965 Laing, W.P., 2004, Tension vein arrays in progressive shear: complex but predictable
966 architecture, and major hosts of ore deposits: Journal of Structural Geology, v. 26, p.
967 1303-1315.
968 Law, B.E., Ulmishek, G.F., and Slavin, V.I., editors, 1998, Abnormal pressure in hydrocarbon
969 environments: AAPG Memoir, v. 70 264 pp.
970 Lisle, R.J., and Vandycke, S., 1996, Separation of multiple stress events by fault striation
971 analysis: an example from Variscan and younger structures at Ogmore, South Wales:
972 Journal of the Geological Society, v. 153, p. 945-953.
973 le Métour, J., 1988, Géologie del'Autochtone des Montagnes d'Oman: la Fenêtre du Saih Hatat:
974 Ph.D. thesis, Pierre and Marie Curie University, Paris 6, France.
975 Lippard, S. J., 1983, Cretaceous high pressure metamorphism in NE Oman and its relationship to
976 subduction and ophiolite nappe emplacement: Journal of the Geological Society of
977 London, v. 140, p. 97-104.
978 Loosveld, R. J. H., Bell, A., and Terken, J. J. M., 1996, The tectonic evolution of interior Oman:
979 GeoArabia, v. 1, p. 28-51.
980 Mann, A., Hanna, S.S. and Nolan, S.C., 1990, The post-Campanian tectonic evolution of the
981 Central Oman Mountains: Tertiary extension of the Eastern Arabian Margin, *in*
982 Robertson, A.H.F., Searle, M.P., and Ries, A.C., editors, The Geology and Tectonics of
983 the Oman Region: Geological Society of London Special Publication, v. 49, p. 549-563.
984 Marzouk, I., and M.A. Sattar, 1995, Wrench tectonics in Abu Dhabi, United Arab Emirates. In,
985 M.I. Al-Husseini (Ed.), Middle East Petroleum Geosciences Conference, GEO'94: Gulf
986 PetroLink, Bahrain, v. 2, p. 655-668.

987 Masse, J.-P., Borgomano, J., and Al Maskiry, S., 1997, Stratigraphy and tectonosedimentary
988 evolution of a late Aptian-Albian carboante margin: the northeastern Akdhar (Sultanate
989 of Oman): Sedimentary Geology, v. 113, p. 269-280.
990 Masse, J.-P., Borgomano, J., and Al Maskiry, S., 1998, A platform-to-basin transition for lower
991 Aptian carbonates (Shuaiba Formation) of the northeastern Jebel Akhdar (Sultanate of
992 Oman): Sedimentary Geology, v. 119, p. 297-309.
993 Miller, J.M., Gray, D.R., and Gregory, R.T., 1998, Exhumation of high-pressure rocks in
994 northeastern Oman: Geology, v. 26, p. 235-238.
995 Mount, V.S., Crawford, R.I.S., and Bergman, S.C., 1998, Regional structural style of the central
996 and southern Oman mountains: Jebel Akhdar, Saih Hatat, and the northern Ghaba Basin.
997 GeoArabia, V. 3, p. 475-490.
998 Nolan, S. C., Skelton, P. W., Clissold, B. P., and Smewing, J. D., 1990, Maastrichtian to early
999 Tertiary stratigraphy and palaeogeography of the central and northern Oman Mountains,
1000 *in* Robertson, A. H. F., Searle, M. P., and Ries, A. C., editors, The Geology and Tectonics
1001 of the Oman Region: Geological Society of London Special Publication, v. 49, p. 495-
1002 519.
1003 Nordgard Bolas, H.M., Hermanrud, C., and Teige, G.M.G., 2004, Origin of overpressures in
1004 shales: constraints form basin modeling: AAPG Bulletin, v. 88, p. 193-211.
1005 Passchier, C.W., and Trouw, R.A.J., 2005, Microtectonics (2nd enlarged edition): Springer
1006 Verlag, Berlin.
1007 Patton, T.L., and O'Connor, S.J., 1986, Cretaceous flexural history of the northern Oman
1008 mountain foredeep, United Arab Emirates. In, Hydrocarbon Potential of Intense Thrust
1009 Zones, Abu Dhabi Conference 1986, v. 1, p. 75-120.
1010 Pearce, J. A., Alabaster, T., Shelton, A. W., and Searle, M. P., 1981, The Oman Ophiolite as a
1011 Cretaceous Arc-Basin Complex: Evidence and Implications: Philosophical Transactions
1012 of the Royal Society of London, Series A, Mathematical and Physical Sciences, v. 300, p.
1013 299-317.
1014 Pillevuit, A., Marcoux, J., Stampfli, G., and Baud, A., 1997, The Oman Exotics: A key to the
1015 understanding of the Neotethyan geodynamic evolution: Geodinamica Acta, v. 10, p.
1016 209-238.

1017 Poupeau, G., Saddiai, O., Michard, A., Goffe, B., and Oberhänsli, R., 1998, Late thermal
1018 evolution of the Oman Mountains subophiolitic windows: apatite fission-track
1019 thermochronology: Geology, v. 26, p. 1139-1142.
1020 Pratt, B. R., and J. D. Smewing, 1993, Early Cretaceous platform margin, Oman, eastern Arabian
1021 Peninsula, *in* Simo, J. A. I., R. W. Scott, and J.-P. Masse, editors, Cretaceous Carbonate
1022 Platforms: American Association of Petroleum Geologists Memoir, v. 56, p. 201-212.
1023 Rabu, D., Nehlig, P., Roger, J., Béchennec, F., Beurrier, M., le Métour, J., Bourdillon-de-
1024 Grissac, C., Tegyey, M., Chauvel, J. J., Cavelier, C., Al Hazri, H., Juteau, T., Janjou, D.,
1025 Lemière, B., Villey, M., and Wyns, R., 1993, Stratigraphy and structure of the Oman
1026 Mountains: (BRGM ed.). Doc. BRGM Orléans, 262.
1027 Ramsay, J.G., 1980, The crack-seal mechanism of rock deformation: Nature v. 284, p. 135-139.
1028 Ramsay, J. F., and Huber, M. I. 1983, The techniques of modern structural geology: Academic
1029 Press, London.
1030 Ramsay, J. G., and Lisle, R. J., 2000, The Techniques of Modern Structural Geology. Volume 3:
1031 Applications of Continuum Mechanics in Structural Geology: London, Academic Press.
1032 Reif, D., Decker, K., Grasemann, B., and Peresson, H., 2012, Fracture patterns in the Zagros
1033 fold-and-thrust belt, Kurdistan Region of Iraq: Tectonophysics, v. 576-577, p. 46-62.
1034 Richard, P.D., Naylor, M.A., and Koopman, A., 1995, Experimental models of strike-slip
1035 tectonics: Petroleum Geoscience, v. 3, p. 71-80.
1036 Richard, P., Bazalgette, L., and Al-Kindi, M., 2014, North Oman fault geometries in outcrops,
1037 analogues and subsurface, in Rollinson, H. R., Searle, M. P., Abbasi, I. A., Al-Lazki, A.,
1038 and Al Kindi, M. H., editors, Tectonic Evolution of the Oman Mountains: Geological
1039 Society of London Special Publication, v. 392, p. 447-460.
1040 Roering, C., 1968, The geometrical significance of natural en-echelon crack-arrays:
1041 Tectonophysics, v. 5, p. 107-123.
1042 Roger, J., Béchennec, F., Janjou, D., le Métour, J., Wyns, R., and Beurrier, M., 1991, Geological
1043 map of the Ja'Alan Quadrangle, Sultanate of Oman. Geoscience map, scale 1:100,000,
1044 sheet NF 40-8E and explanatory notes, Ministry of Petroleum and Minerals, Directorate
1045 General of Minerals, Sultanate of Oman, 90 p.
1046 Searle, M. P., 1985, Sequence of thrusting and origin of culminations in the northern and central
1047 Oman Mountains: Journal of Structural Geology, v. 7, p. 129-143.

1048 Searle, M. P., 2007, Structural geometry, style and timing of deformation in the Hawasina
1049 Window, Al Jabal al Akhdar and Saih Hatat culminations, Oman Mountains: GeoArabia,
1050 v. 12, p. 99-130.
1051 Searle, M. P., and Graham, G. M., 1982, "Oman Exotics" - oceanic carbonate build-ups
1052 associated with the early stages of continental rifting: Geology, v. 10, p. 43-49.
1053 Searle, M. P., and Malpas, J., 1980, Structure and metamorphism of rocks beneath the Semail
1054 Ophiolite of Oman and their significance in ophiolite obduction: Transactions of the
1055 Royal Society of Edinburgh, Earth Sciences, v. 71, p. 247-262.
1056 Searle, M. P., and Malpas, J., 1982, Petrochemistry and origin of sub-ophiolite metamorphic and
1057 related rocks in the Oman Mountains: Journal of the Geological Society of London, v.
1058 139, p. 235-248.
1059 Searle, M. P., Warren, C. J., Waters, D. J., and Parrish, R. R., 2004, Structural evolution,
1060 metamorphism and restoration of the Arabian continental margin, Saih Hatat region,
1061 Oman Mountains: Journal of Structural Geology, v. 26, p. 451-473.
1062 Secor, D.T., 1965, Role of fluid pressure in jointing: American Journal of Science, v. 263, p.
1063 633-646.
1064 Sharland, P.R., Casey, D.M., Davies, R.B., Simmons, M.D., and Sutcliffe, O.E., 2004, Arabian
1065 Plate Sequence Stratigraphy. GeoArabia, v. 9, no. 1, p. 199-214.
1066 Srivastava, D.C., 2000, Geometrical classification of conjugate vein arrays: Journal of Structural
1067 Geology, v. 22, p. 713-722.
1068 Stark, L., 2011, Geostatistical analysis of vein systems in the Jabal Akhdar dome, Oman: M.Sc
1069 thesis, Eberhard Karls University of Tübingen, Germany.
1070 Staude, S., Bons, P.D., and Markl, G., 2009, Hydrothermal vein formation by extension-driven
1071 dewatering of the middle crust: An example from SW Germany: Earth and Planetary
1072 Science Letters, v. 286, p. 387-395.
1073 Swarbrick R.E., and Osborne, M.J., 1998, Mechanisms that generate abnormal pressures: an
1074 overview. In: Abnormal Pressures in Hydrocarbon Environments, *in* Law, B.E.,
1075 Ulmishek, G.F., and Slavin, V.I., editors, AAPG Memoir, v. 70, pp. 13-33.
1076 Tavani, S., Mencos, J., Bausà, J., and Muñoz, J. A., 2011, The fracture pattern of the Sant
1077 Corneli Bóixols oblique inversion anticline (Spanish Pyrenees): Journal of Structural
1078 Geology, v. 33, p. 1662-1680.

Van Noten, K., Muchez, P., and Sintubin, M., 2011, Stress-state evolution of the brittle upper crust during compressional tectonic inversion as defined by successive quartz vein types (High-Ardenne slate belt, Germany): Journal of the Geological Society, London, v. 168, p. 407-422.

Van Noten, K., Muchez, P., and Sintubin, M., 2012, The complexity of 3D stress-state changes during compressional tectonic inversion at the onset of orogeny: Geological Society, London, Special Publications, v. 367, p. 51-69.

Virgo, S., Arndt, M., Sobisch, Z., and Urai, J.L., 2013a, Development of fault and vein networks in a carbonate sequence near Hayl al-Shaz, Oman Mountains: GeoArabia, v. 18, p. 99-136.

Virgo, S., Abe, S., and Urai, J.L., 2013b, Extension fracture propagation in rocks with veins: Insight into the crack-seal process using Discrete Element Method modeling: Journal of Geophysical Research: Solid Earth, v. 118, p. 5236-5251.

Warburton, J., Burnhill, T. J., Graham, R. H., and Isaac, K. P., 1990, The evolution of the Oman Mountains Foreland Basin, *in* Robertson, A. H., Searle, M. P., and Ries, A. C., editors, The Geology and Tectonics of the Oman Region, Geological Society of London Special Publication, v. 49, p. 419-427.

Warren, C. J., Parrish, R. R., Searle, M. P., and Waters, D. J., 2003, Dating the subduction of the Arabian continental margin beneath the Semail Ophiolite, Oman: Geology, v. 31, p. 889-892.

Weisheit, A., Bons, P.D., and Elburg, M.A., 2013, Long-lived crustal-scale fluid-flow: The hydrothermal mega-breccia of Hidden Valley, Mt. Painter Inlier, South Australia: International Journal of Earth Sciences, v. 102, p. 1219-1236.

Ziegler, M. A., 2001, Late Permian to Holocene Paleofacies evolution of the Arabian Plate and its hydrocarbon occurrences: GeoArabia, v. 6, p. 445-503.

Figure captions

Fig. 1. (A) Geological map of the central part of the Oman Mountains. The Jabal Akhdar and Saih Hatat tectonic windows expose rocks of the Autochthons A and B. (B) NE-SW cross-section. Figure (A) is modified from Breton and others (2004), who compiled it from the

Geological Map of Oman, scale 1:1,000,000 (Le Métour and others, 1993). Figure (B) is modified from Searle (2007).

Fig. 2. Simplified lithostratigraphic column of the Autochthonous B units of the Jabal Akhdar area. The log is modified from the Geological Map of Seeb, scale 1:250,000 (Béchennec and others, 1992). The ages of the formations are from figure 2 of Breton and others (2004).

Fig. 3. Simplified map of the western part of the Jabal Akhdar dome. Squares with numbers indicate the location of the areas used for this study. Dashed lines are rivers or water streams that define wadis (valleys). A complete list of localities with coordinates is shown in table 1. Figure compiled from the Geological Map of Oman (Rustaq sheet), scale 1:100,000 (Beurrier and others, 1986). Locality 12 is out of the map. Thin lines indicate fault traces. The geographical coordinates of the upper left corner are (57º00'E, 23º30'N).

Fig. 4. Sketches summarizing the methods to estimate stress orientations from different structures. (A) Faults with striations (dip-slip, strike-slip and oblique-slip). (B) Conjugate sets of hybrid or shear veins. (C) Tectonic stylolites. (D) Slickenfibres or striations on layer-parallel veins. (E) Sketches showing the typical vein cross-cutting relationships found in the field (e.g. Virgo and others, 2013b).

Fig. 5. Structures of event *#1*. (A) Plot summarizing formation depth of sedimentary stylolites. Arrows point towards the stratigraphic position and unit from where they were collected. (B) Bedding-confined calcite veins with lenticular shape in cross-section. (C) Calcite-filled veins confined to dm-scale beds. Both images show rocks of the Natih Fm. These veins are consistently rotated with bedding due to top-to-the-South thrusting event, which corresponds to event *#2*. Photographs (A) and (B) were taken at locality 13, and locality 14, respectively.

Fig. 6. Structures of event *#2*. (A) Slickenfibres on shallow-dipping veins indicating top-to-the-South sense of layer-parallel shearing in limestones. (B) Detail of photo (A). The diameter of the 1-cent Euro coin is 16.25 mm. (C) Summary of the orientations of slickenfibres on layer-parallel veins at the three localities where they were found. Each dot represents an individual

1141 measurement. Note that the original data have been rotated in this plot assuming that layers were
1142 horizontal when the structures developed. (D) Stepped layer-parallel vein showing top-to-South
1143 movement.
1144
1145 **Fig. 7.** Structures of event *#3*. (A) Conjugate normal faults in the Nahr Umr Fm. (B) detail of
1146 vertical striations on the right normal fault of photo (A). (C) One set of normal faults filled with
1147 calcite in limestones of the Shams Fm. (D) detail of vertical striations on fault plane of photo
1148 (C). (E) View of an outcrop in the Natih Fm with conjugate sets of *en-échelon* and sigmoidal
1149 veins formed due to a σ_1 perpendicular to layers (i.e. subvertical). (F) Normal fault (event *#3*)
1150 offsetting a layer-parallel vein with a top-to-S sense of shearing (event *#2*). (G) Summary of the
1151 orientations of principal compression stresses σ_1 and σ_3 at the localities where these structures
1152 were found. Each square represents the average of measurements at each outcrop. Note that the
1153 original orientation data have been rotated in this plot assuming that layers were horizontal when
1154 these structures formed. (H) Detail of photo (F).
1155
1156 **Fig. 8.** Structures of event *#3*, probably reactivated by younger events (*#5*, *#6*, *#7*). (A) Large-
1157 scale dip-slip fault with a stratigraphic offset of ~700 m. (B) Large-scale dip- to oblique-slip
1158 fault that was later reactivated in strike-slip. (C) The damage zones of some of these faults are
1159 containing numerous calcite veins, probably formed during subsequent strike-slip events. (D-E-
1160 F) Details of breccias found in the damage zones of one of these large-scale faults. In photo (E),
1161 which is oriented W-E, a tectonic stylolite is dissolving the interface between the breccia and the
1162 host rock, indicating that the breccia formed before the stylolite. (F) Microphotograph of the
1163 fault breccia, taken under plane polarized light.
1164
1165 **Fig. 9.** Effects of event *#4*. (A) S-N view of top-the-Northeast shearing of the normal faults of
1166 figure 7A-B (Nahr Umr Fm). (B) Detail of layer-parallel striations pointing towards the
1167 Northeast. (C) Detail of top-to-the-northeast layer-parallel shearing. (D) Sigmoidal calcite veins
1168 sheared towards the NE (Shams Fm). (E) Summary of the orientations of striations and
1169 slickenfibres directions at the six localities were layer- and cleavage-parallel veins with a NE
1170 shearing direction were found (event *#4*). Each dot represents the average of measurements at

each outcrop. Note that original orientations have been rotated in this plot considering that layers were horizontal when these structures were formed.

Fig. 10. (A) Vein of event *#5* with subhorizontal slickenfibres crystals. (B) *en-échelon* conjugate sets of veins of event *#6a* (E-W-compression oriented) crosscutting veins of event *#5* (NW-SE-compression oriented). (C) *en-échelon* veins of event *#6b* (NNE-SSW-oriented compression) crosscutting veins of event *#5*. (D-E) Examples of cross-cutting relationships between the different strike-slip vein sets. A stylolite dissolves the center of a vein of event *#6b*. (F) E-W-oriented large-scale fault with two sets of striations indicating older dip-slip and younger strike-slip movements. (G) Microphotograph showing the typical crack-seal microstructures of veins of the three strike-slip events. These veins are generally formed by hundreds or thousands of micro-crack events. This photo illustrates the transition from distributed to localized crack-sealing of a vein of event *#6b*. (H-I) Summary of the orientations of principal compression stresses σ_1 and σ_3 at the localities were the structures of events *#5*, *#6* and *#7* were measured. Each square represents the average of measurements at each outcrop. Nota that the original orientations have been rotated in this plot assuming that layers were horizontal when these structures were formed. The structures shown in all these photos are all from rocks of the Natih Fm.

Fig. 11. (A) Detail of a tectonic stylolite (developed during stage *#6*) dissolving a vein of event *#5*. (B) Tectonic stylolites dissolving dip-slip and strike-slip striations on a large-scale fault plane. (C) Complex relationships between structures: tectonic stylolite dissolves a calcite vein of event *#5* and the same vein crosscuts tectonic stylolites. (D) bedding-parallel stylolites cutting a vein of event *#5*. (E) Stereoplot showing the data collected from tectonic stylolites in the southern limb of the Jabal Akhdar area. Figure displays pole plots and Kamb contours indicating two maximum compression directions: NW-SE (event *#5*) and E-W (event *#6*). A total of 41 measurements are displayed in this plot. White triangles show the average orientations of σ_1 calculated from tectonic stylolites of both sets. For comparison, black squares indicate the average orientations of σ_1 for the sets of fractures and veins of events *#5* and *#6*.

Fig. 12. (A, B) Sets of joints of different scales in the Natih Fm. (C) Thin and straight veins in the Natih Fm. (D) Orientations of joints and associated thin veins. Each great circle represents

the average orientation calculated at one outcrop. These orientations are compatible with the present-day stress field in Oman.

Fig. 13. Sketches summarizing the structural evolution of the Jabal Akhdar dome, with the order of identified events and calculated stress fields orientations. The stereogram illustrates the evolution of σ_1 showing two main trends: firstly obduction (*#2*), normal (dip-slip) and oblique-slip faulting (*#3*), reverse thrusting and exhumation (*#4*), and secondly a far horizontal σ_1 that comprises three events (*#5* to *#7*). It is possible that event #3 did not form after obduction but before it.

Fig. 14. Sketches and Mohr circles illustrating the effect of effective fluid pressure increase on the onset of fracture/vein sets. (A) Shows the definition of normal (σ_n) and shear (σ_s) stresses. An increase in effective fluid pressure (from (D) to (B)) shifts the Mohr circle to the left. This effect enhances failure and the onset of fractures with a higher angle of internal friction (ϕ) and lower angle between conjugate sets (α). (B) High fluid pressures lead to the onset of only one set parallel to σ_1. (C) A relative high friction angle leads to two conjugate sets of hybrid fractures/veins with a significant opening component. (D) A smaller friction angle favors the onset of two conjugate sets of fractures/veins with a significant shear component. If these veins are segmented, individual segments have a significant opening component. Note that the angle α is double in the Mohr circle (ζ).

Fig. 15. Graphs showing the acute angles between mean orientations of conjugate sets (α) of fractures and veins versus stratigraphic position (related to depth) of the structures (see fig. 2). The data is organized by tectonic events. Note that the only event where there is a significant trend of conjugate angles (hence angle of internal friction or effective fluid pressure) is event *#6*. In this case conjugate angles (α) increase with depth. The lowest values occur at the Natih Fm, just below the Muti Fm. The relative thickness of each formation is not displayed in the graph, so that the *Y*-axis does not have a scale.

Tables

Table 1. List of the areas used for this study. Note that locality 12 is out of the map of figure 3. Coordinates are in decimal degrees.

Table 2. Summary of datasets collected at each outcrop. Please note that mean σ_1 orientations have been calculated from fracture and vein populations. Striation orientations refer to striations on fault planes or striations and stretched crystal directions on layer-parallel veins. Note that original orientations have been rotated in this plot considering that layers were horizontal when these structures formed, except for those of event *#8* and that of event *#6* at locality 10.

Table 3. Comparison of tectonic events found in this study with those of previous publications.

Gomez-Rivas et al., Figure 1

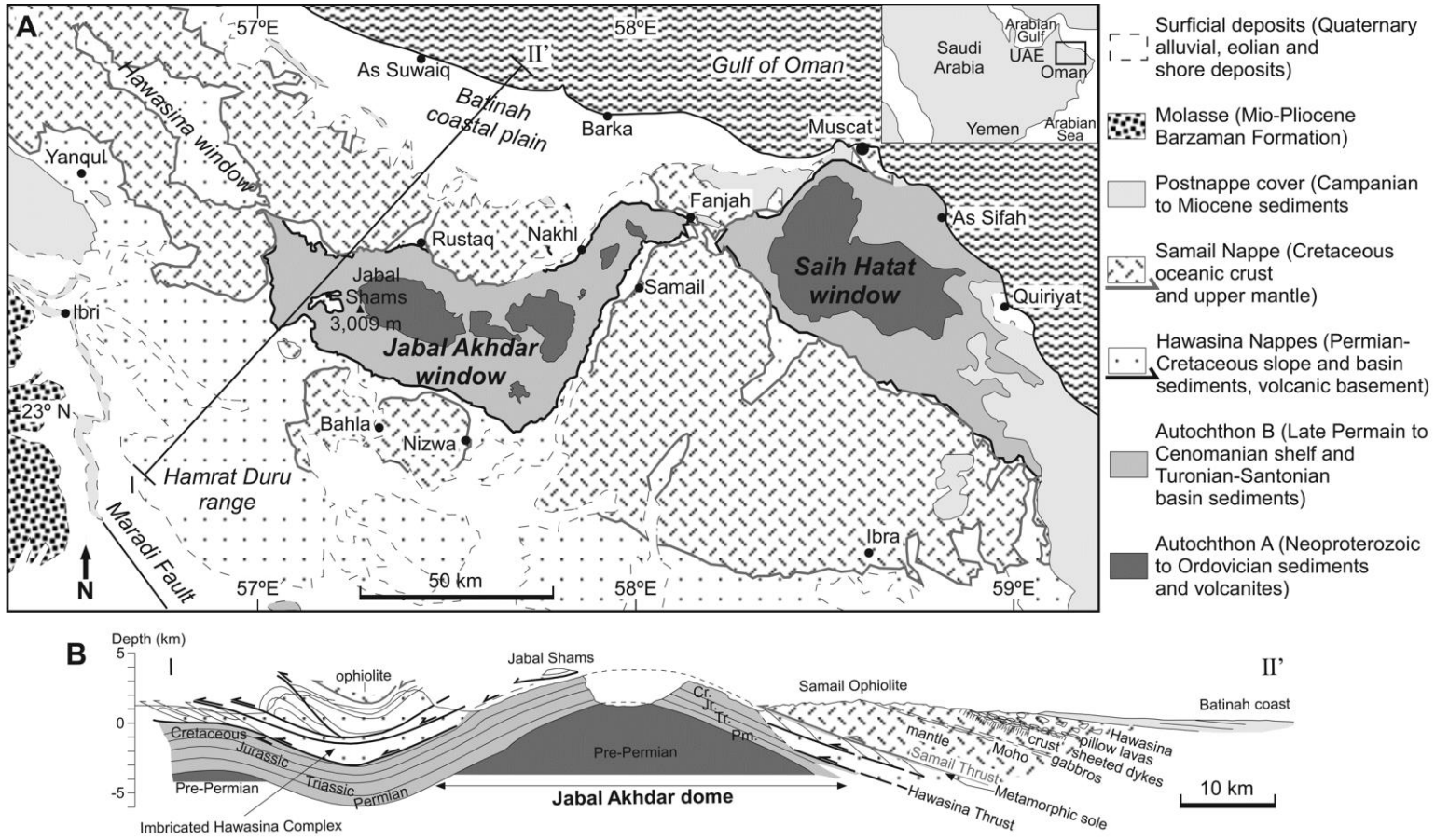

Gomez-Rivas et al., Figure 2

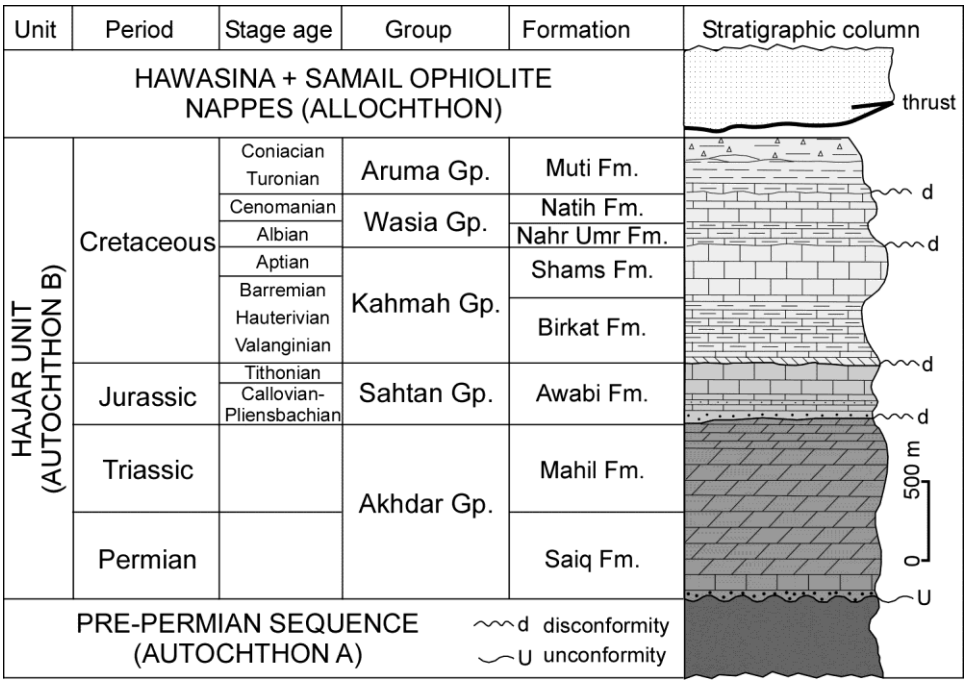

Gomez-Rivas et al., Figure 3

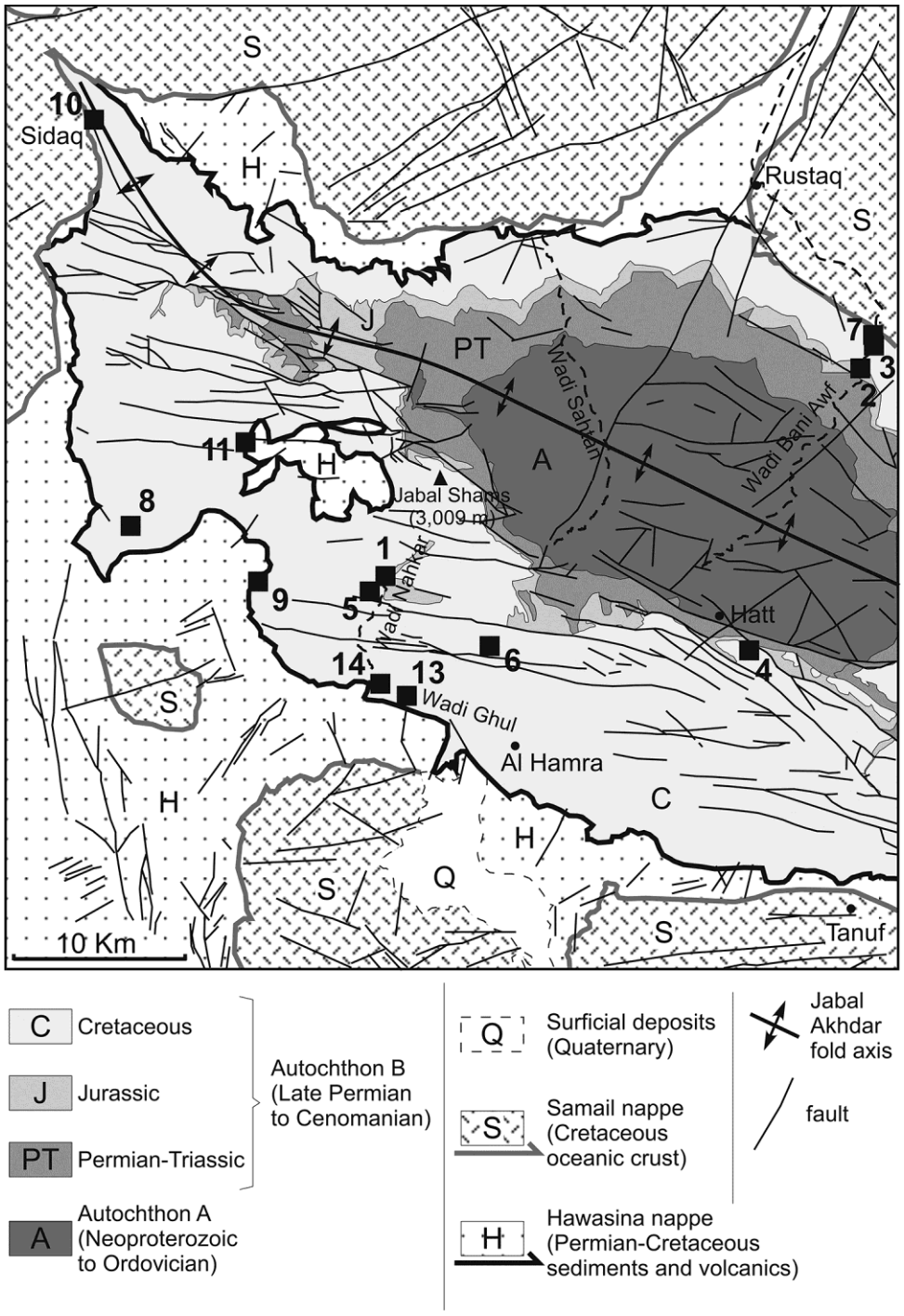

Gomez-Rivas et al., Figure 4

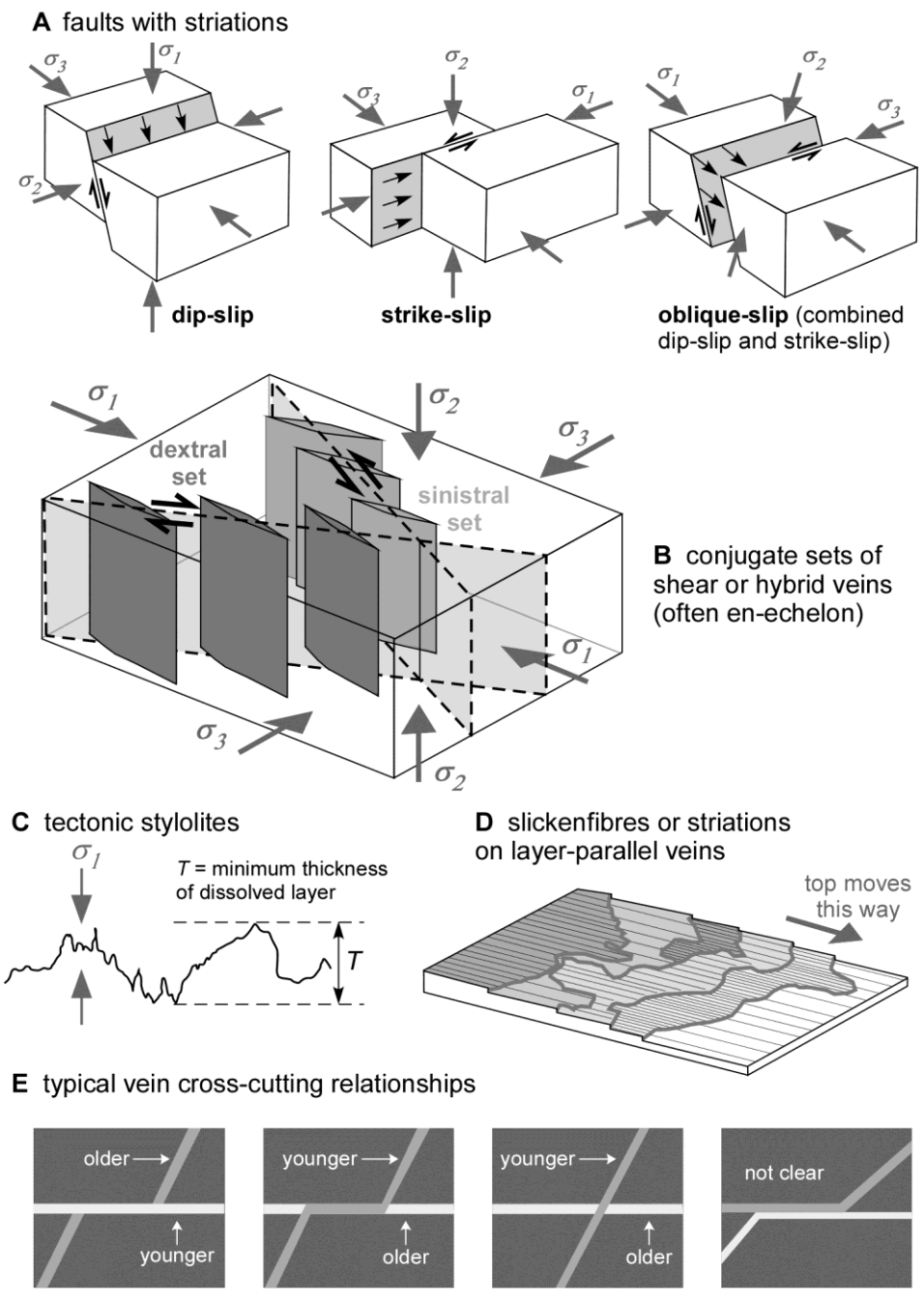

Gomez-Rivas et al., Figure 5

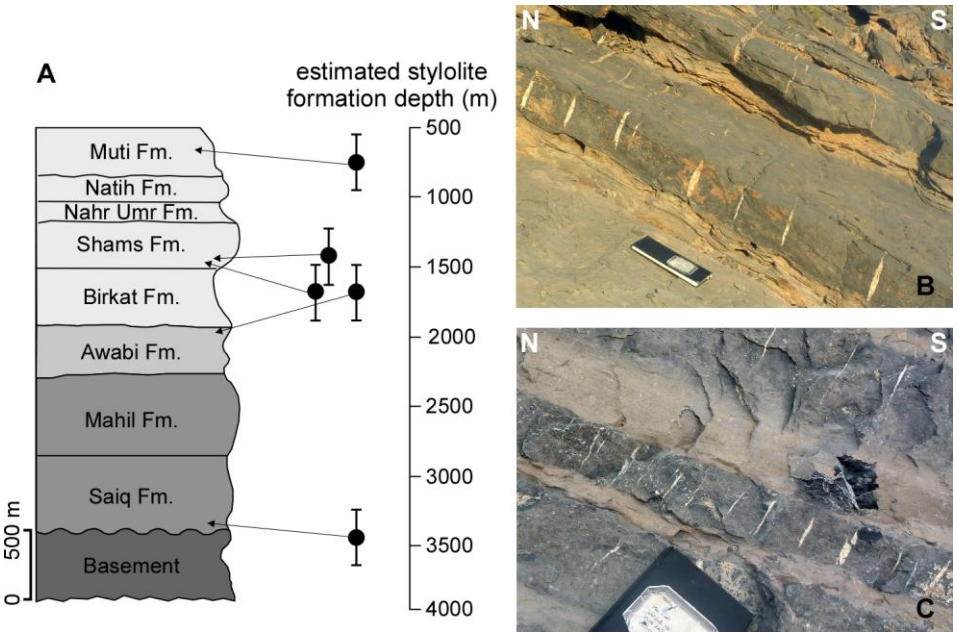

Gomez-Rivas et al., Figure 6

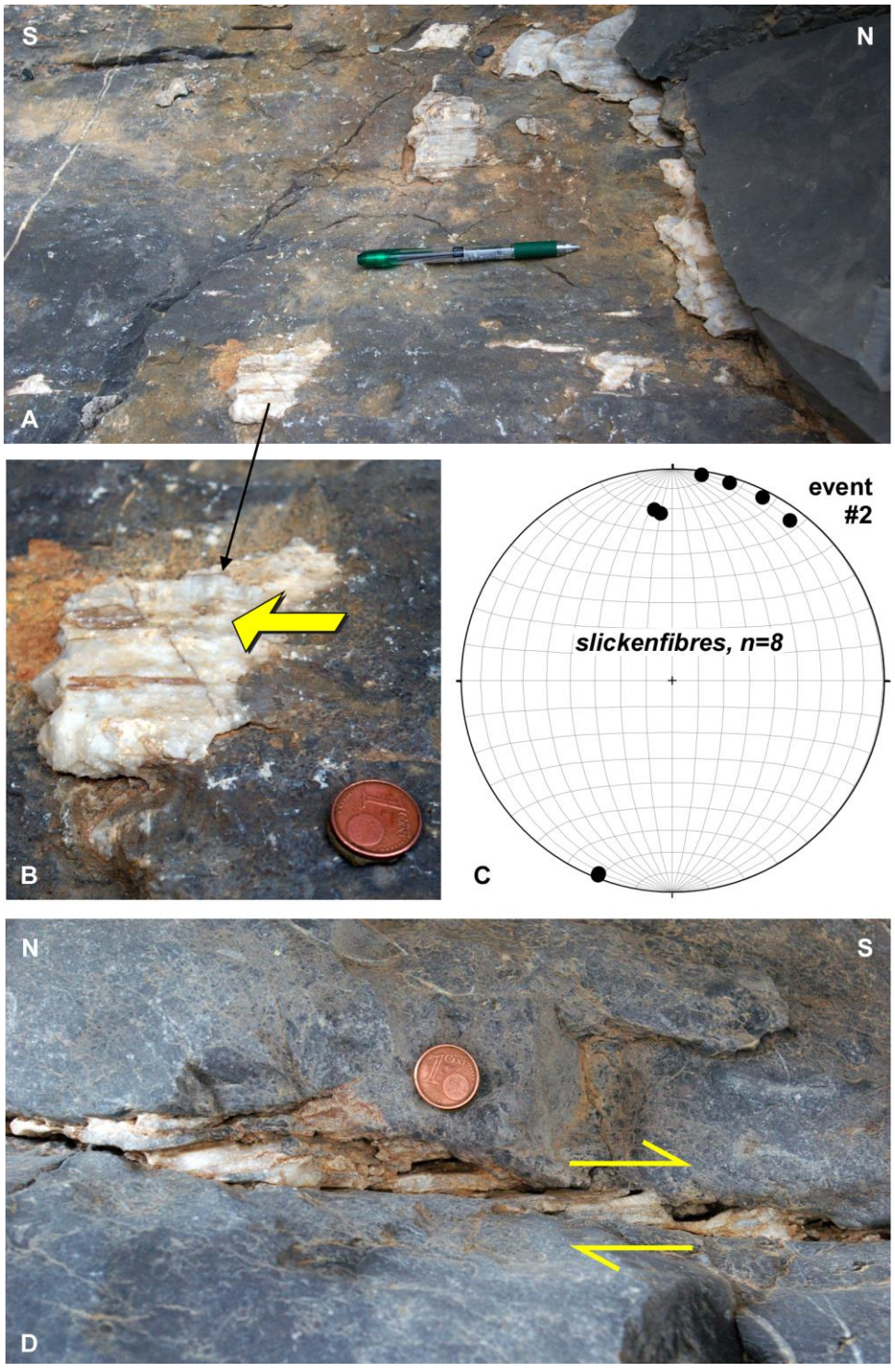

Gomez-Rivas et al., Figure 7

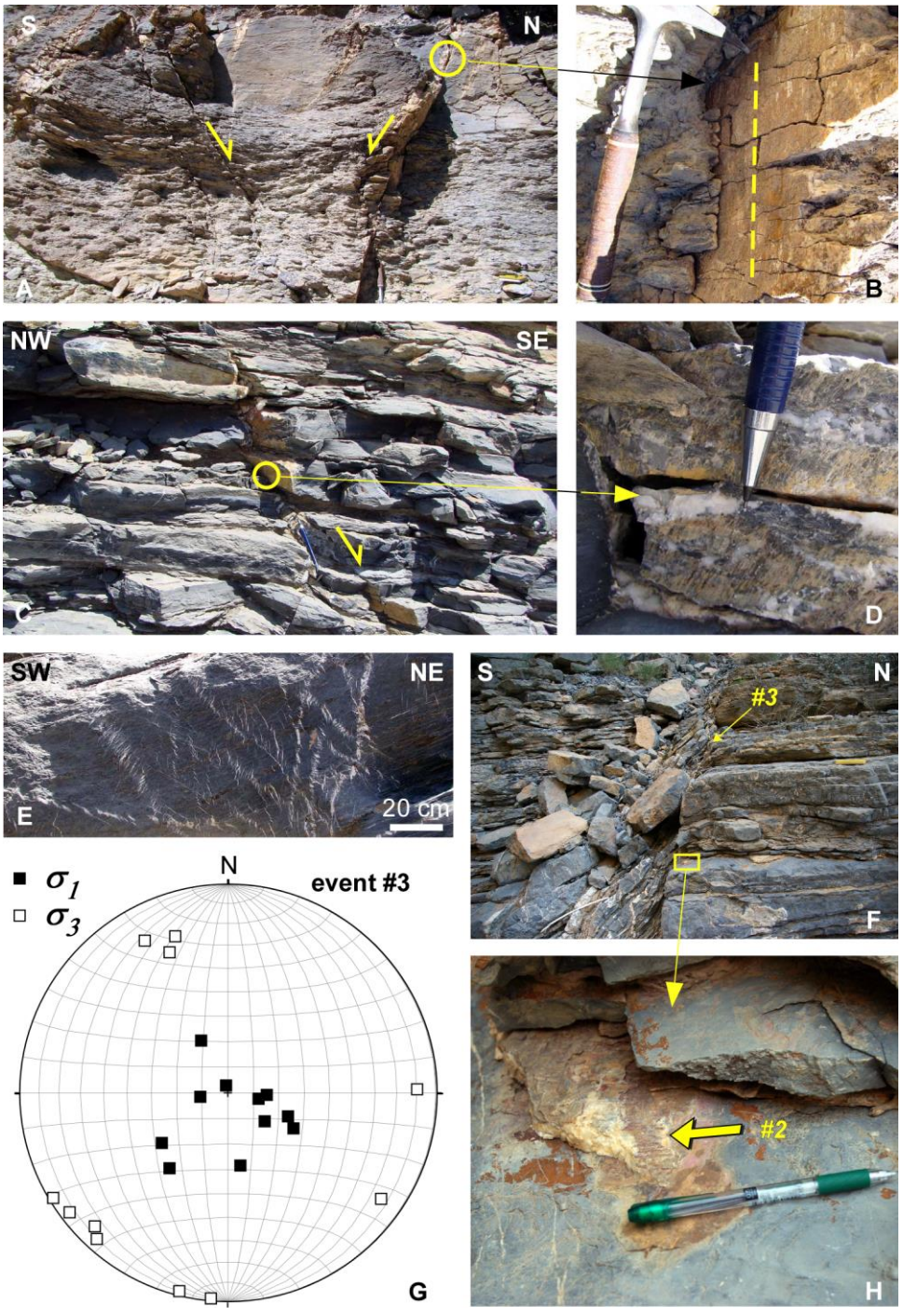

Gomez-Rivas et al., Figure 8

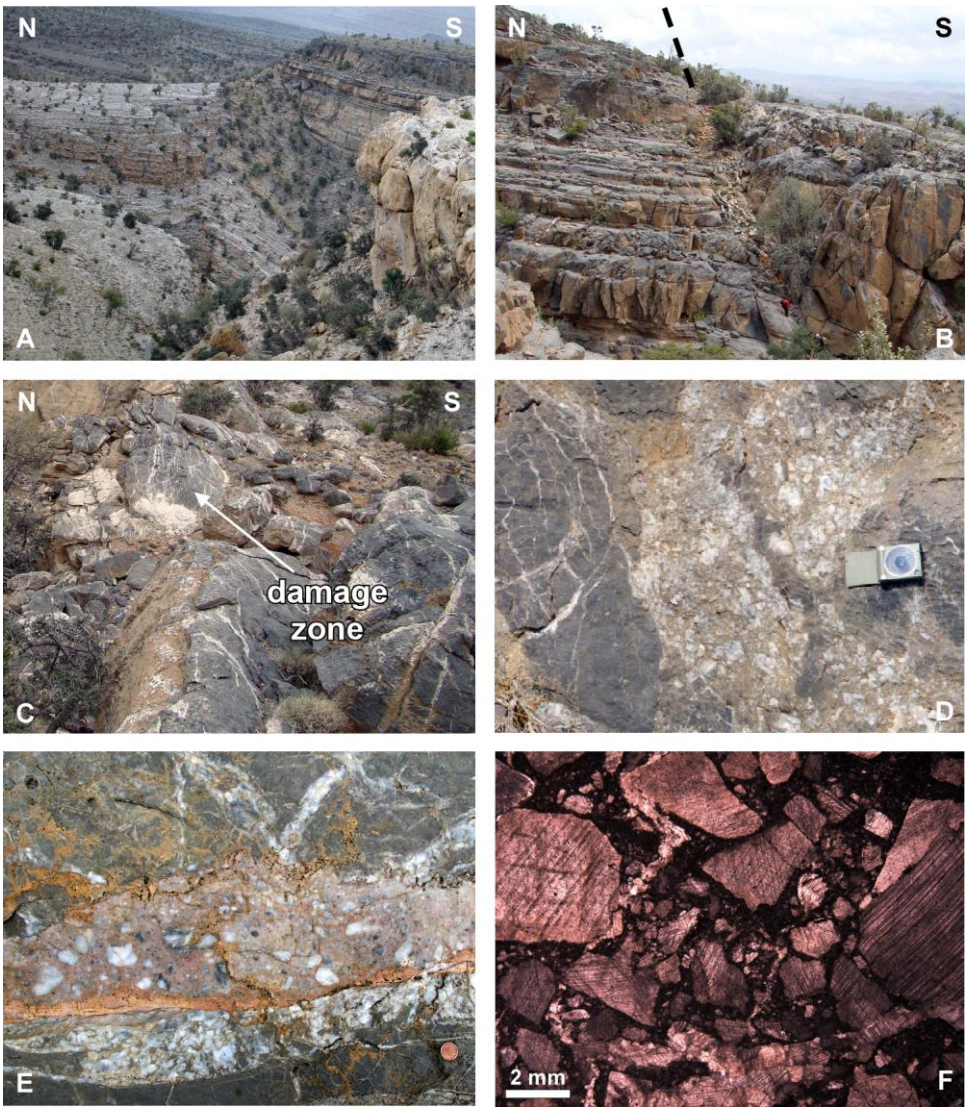

Gomez-Rivas et al., Figure 9

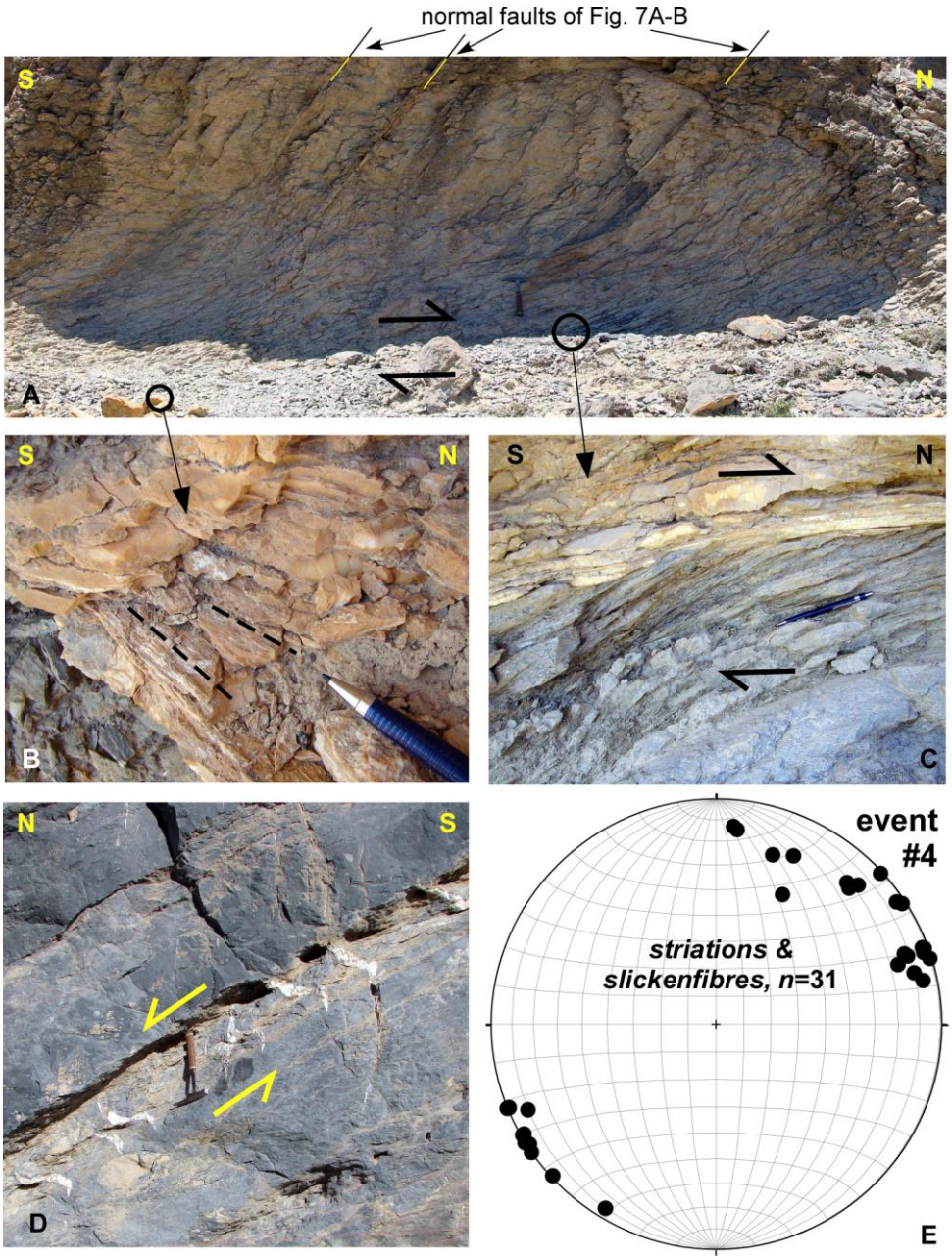

Gomez-Rivas et al., Figure 10

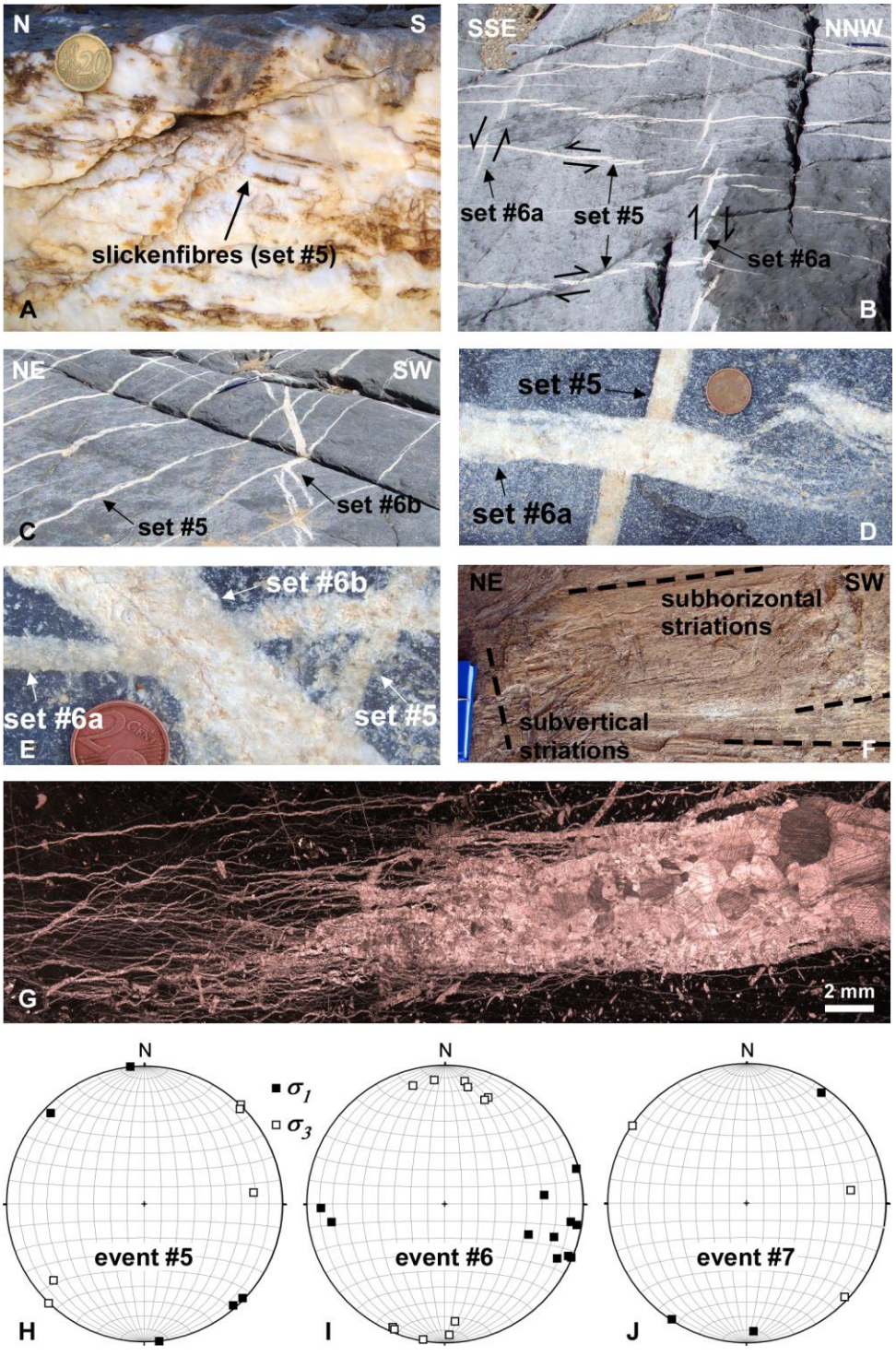

Gomez-Rivas et al., Figure 11

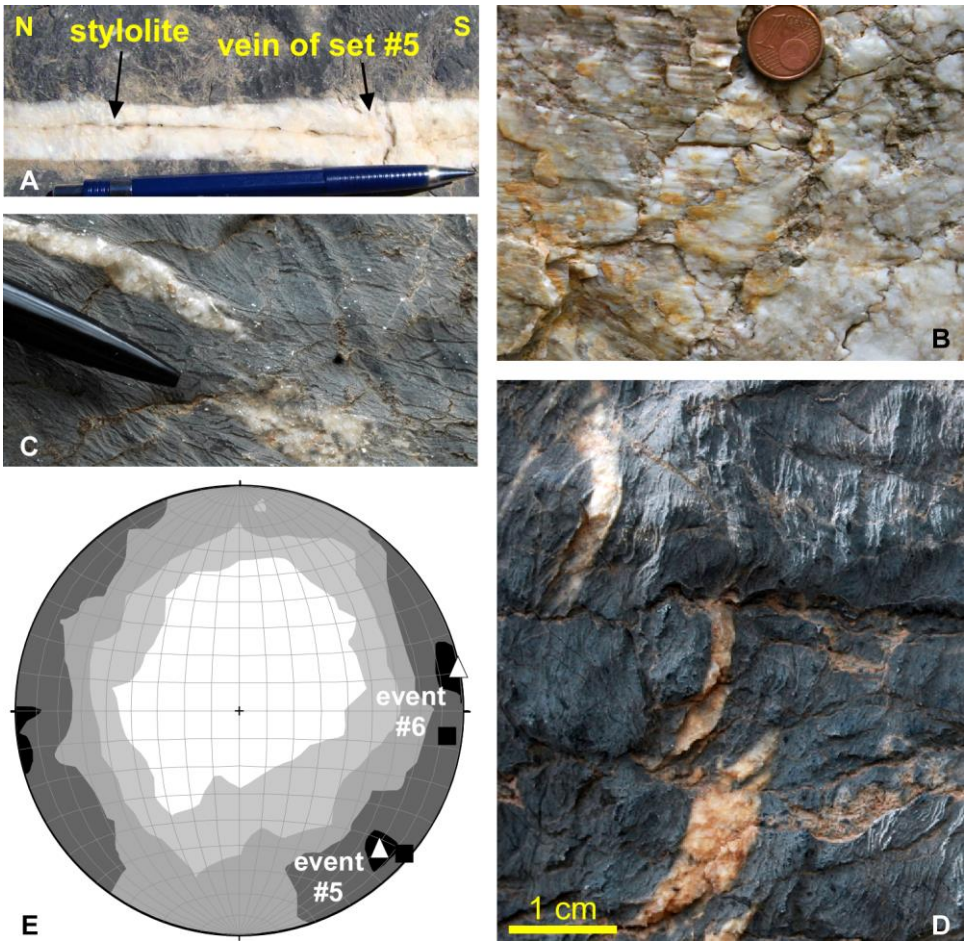

Gomez-Rivas et al., Figure 12

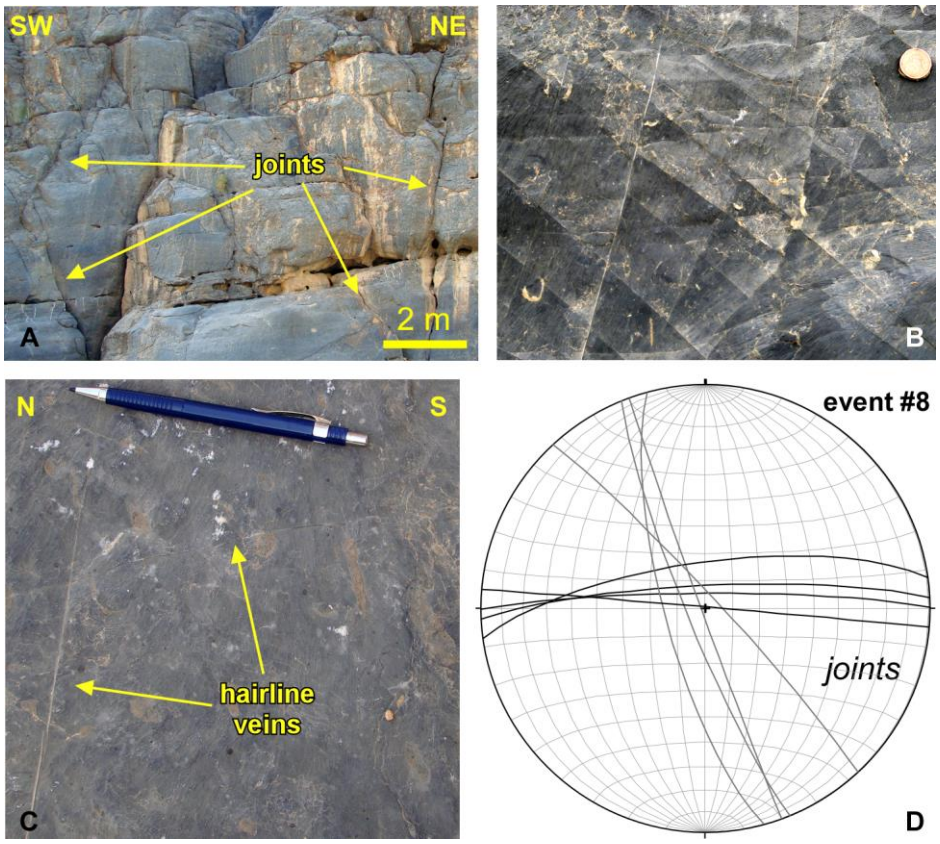

Gomez-Rivas et al., Figure 13

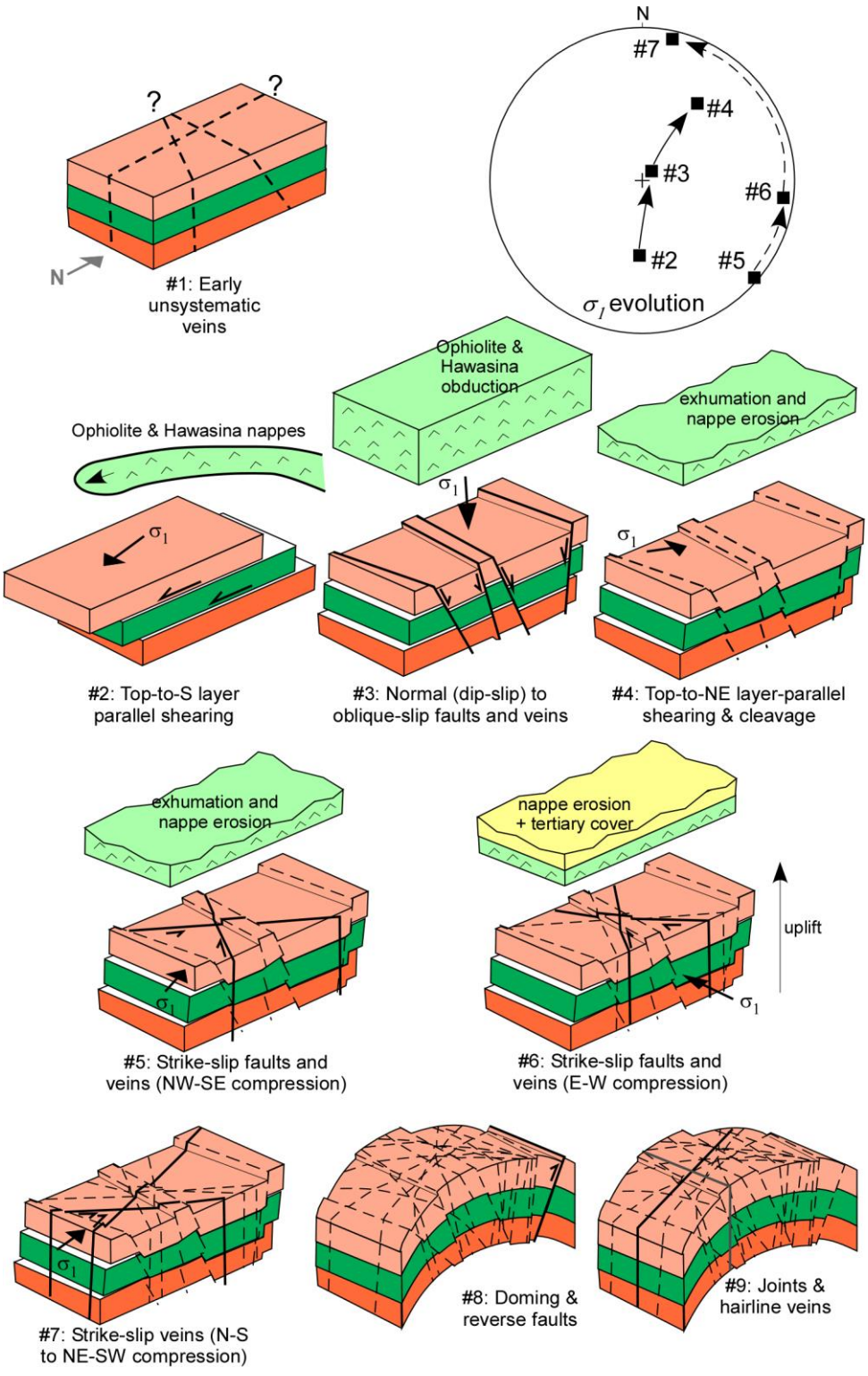

Gomez-Rivas et al., Figure 14

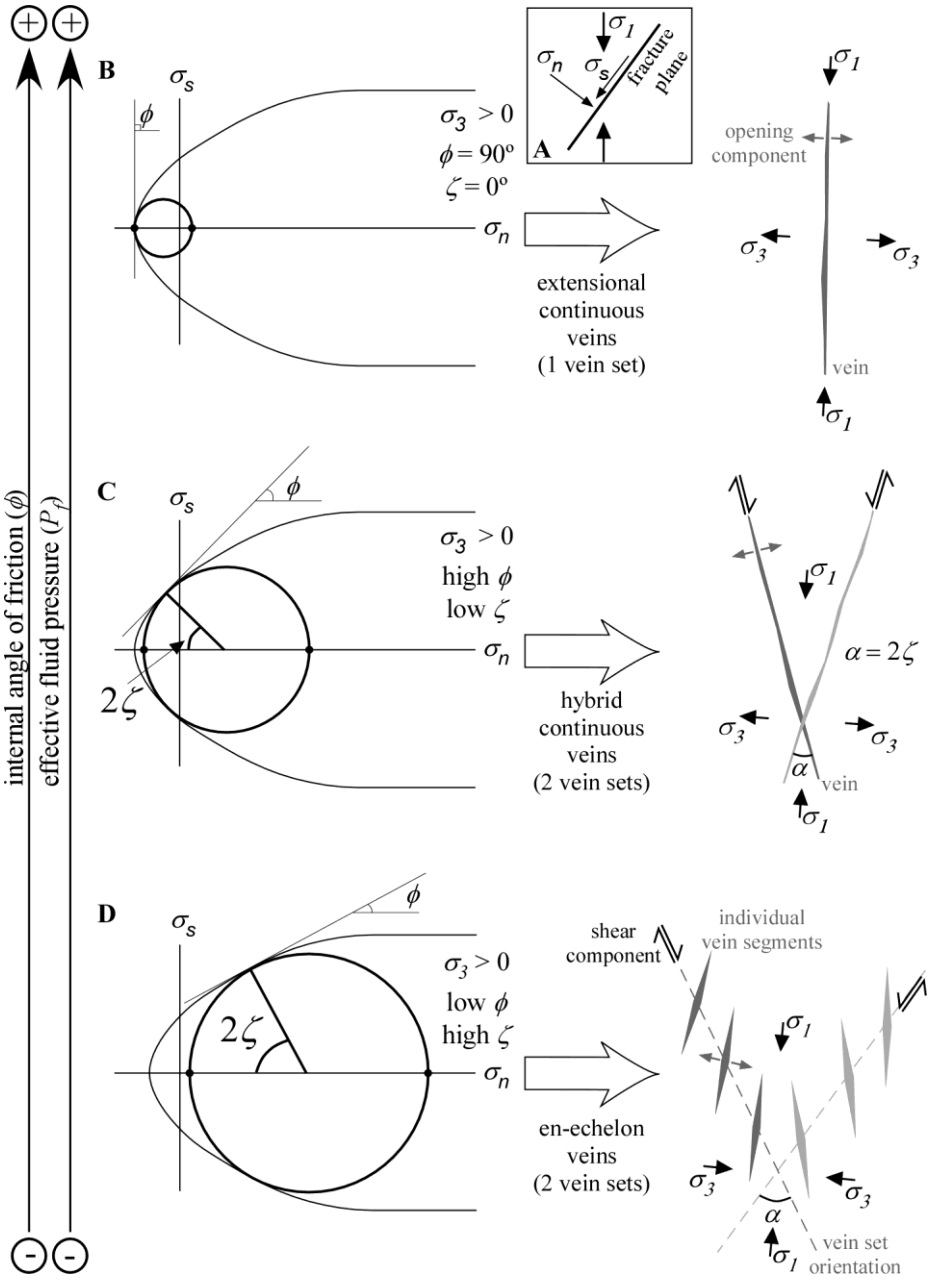

Gomez-Rivas et al., Figure 15

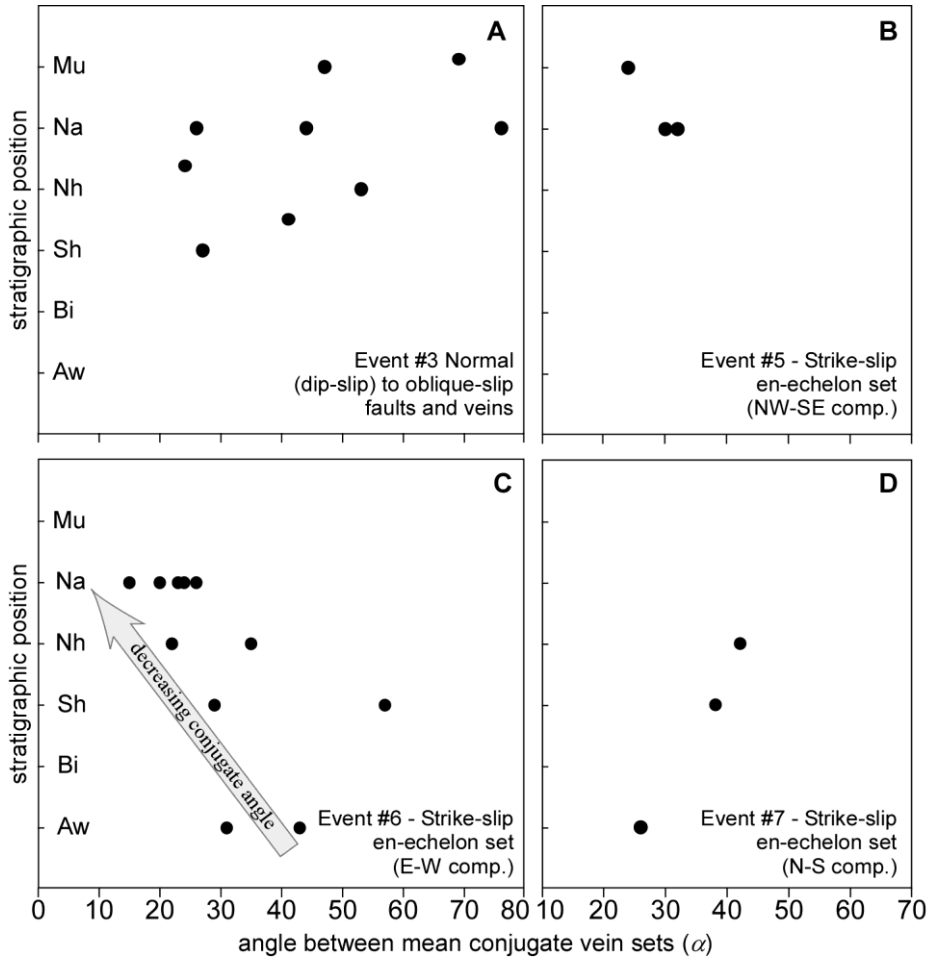

Gomez-Rivas et al., Table 1

Locality		Geographic coordinates		
Number	Name	Latitude	Longitude	host rocks
1	Wadi Nakhar	23.204344 ºN	57.212668 ºE	Sahtan Gp
2	Wadi Bani Awf	23.311712 ºN	57.480088 ºE	Sahtan Gp
3	Wadi Bani Awf	23.323553 ºN	57.487778 ºE	Shams Fm
4	Road Tanuf to Hatt	23.165308 ºN	57.417064 ºE	Shams Fm
5	Top of Wadi Nakhar	23.196403 ºN	57.203803 ºE	Nahr Umr Fm
6	Hayl Al Shaz	23.167877 ºN	57.271193 ºE	Shams and Nahr Umr Fm
7	Wadi Bani Awf	23.329036 ºN	57.487370 ºE	Natih Fm
8	Wadi Dam	23.230574 ºN	57.069394 ºE	Natih Fm
9	Wadi Ghul	23.201594 ºN	57.141022 ºE	Natih Fm
10	Sidaq	23.441775 ºN	57.048858 ºE	Natih Fm
11	"Gorge pavement"	23.273979 ºN	57.134070 ºE	Natih Fm
12	Wadi Halfayn	23.076254 ºN	57.793983 ºE	Muti Fm
13	Wadi Ghul (ramp North of Ghul)	23.151703 ºN	57.221413 ºE	Natih Fm
14	Wadi Nakhr	23.151367 ºN	57.207314 ºE	Natih Fm

Gomez-Rivas et al., Table 2

Locality Number - Name	Host rock (Fm or Gp)	Structures	Number of data	Mean σ_1 or slickenfibre (s.f.) orientation
Event #2 - *top-to-the-South layer-parallel shearing*				
1- Wadi Nakhar	Shams Fm	layer-parallel veins	3	024/04 (s.f.)
6 - Hayl Al Shaz	Shams Fm & Nahr Umr Fm	layer-parallel veins	2	356/21 (s.f.)
8 - Wadi Dam	Natih Fm	layer-parallel veins	3	200/02 (s.f.)
Event #3 - *normal (dip-slip) to oblique-slip faults and veins*				
1 - Wadi Nakhar	Shams Fm	faults& striations	12	093/75 (σ_1)
		faults & striations	6	not calculated (only one set of faults)
4 - Road Tanuf to Hatt	Shams Fm	faults & striations	30	233/57 (σ_1)
		faults& striations	8	not calculated (only one set of faults)
5 - Top of Wadi Nakhar	Nahr Umr Fm	faults, striations & veins	15	343/87 (σ_1)
6 - Hayl Al Shaz Nahr Umr Fm	Shams Fm &	faults & striations	12	213/55 (σ_1)
		faults & striations	4	not calculated (only one set of faults)
7 - Wadi Bani Awf	Natih Fm	faults, striations & veins	4	112/65 (σ_1)
11 - "Gorge pavement"	Natih Fm	veins	12	262/79 (σ_1)
		veins	6	119/62 (σ_1)
		faults & striations	6	not calculated (only one set of faults)
		faults & striations	8	not calculated (only one set of faults)
12 - Wadi Halfayn	Muti Fm	veins	9	101/78 (σ_1)
		veins	4	171/61 (σ_1)
Event #4 - *top-to-the-Northeast layer- and cleavage-parallel veins*				
1 - Wadi Nakhar	Shams Fm	layer-parallel veins	3	034/18 (s.f.)
3 - Wadi Bani Awf	Shams Fm	cleavage - & layer-parallel veins	3	044/15 (s.f.)
4 - Road Tanuf to Hatt	Shams Fm	layer-parallel veins	10	065/01 (s.f.)
5 - Top of Wadi Nakhar	Nahr Umr Fm	cleavage-parallel veins	6	231/03 (s.f.)
8 - Wadi Dam	Natih Fm	layer-parallel veins	6	070/08 (s.f.)
11 - "Gorge pavement"	Natih Fm	layer-parallel veins	3	016/24 (s.f.)
Event #5 - *strike-slip faults and veins with NW-SE-oriented compression*				
8 - Wadi Dam	Natih Fm	veins	37	314/01 (σ_1)
9 - Wadi Ghul	Natih Fm	veins	24	174/00 (σ_1)
12 - Wadi Halfayn	Muti Fm	veins	10	139/04 (σ_1)
		faults	9	314/06 (σ_1)
Event #6 - *strike-slip faults and veins: E-W-oriented principal compression*				
1 - Wadi Nakhar	Sahtan Gp	veins	14	107/19 (σ_1)

Shams Fm		veins	4	113/01 (σ_1)
		faults & striations	12	not calculated (only one set of faults)
2 - Wadi Bani Awf	Sahtan Gp	veins	4	110/36 (σ_1)
3 - Wadi Bani Awf	Shams Fm	veins	31	098/09 (σ_1)
5 - Top of Wadi Nakhar	Nahr Umr Fm	veins	25	113/04
6 - Hayl Al Shaz	Shams & Nahr Umr Fm	faults & striations veins	6	not calculated (only one set of faults)
8 - Wadi Dam	Natih Fm	veins	22	086/26 (σ_1)
9 - Wadi Ghul	Natih Fm	veins (event *#6a*)	18	075/02 (σ_1)
		veins (event *#6b*)	16	116/11 (σ_1)
10 - Sidaq	Natih Fm	veins	12	268/12 (σ_1) (post-folding)
11 - "Gorge pavement"	Natih Fm	veins	16	(σ_1)
		faults & striations	12	not calculated (only one set of faults)

Event #7 - *strike-slip veins: N-S to NE-SW-oriented principal compression*

1 - Wadi Nakhar	Sahtan Gp Shams Fm	veins	9	177/09 (σ_1)
4 - Road Tanuf to Hatt	Shams Fm	veins	14	213/01 (σ_1)
6 - Hayl Al Shaz	Shams & Nahr Umr Fm	veins	12	034/05 (σ_1)

Event #9 - *joints and hairline veins*

1 - Wadi Nakhar	Shams Fm	joints	21	124/11 (σ_1) (post-folding)
8 - Wadi Dam	Natih Fm	joints	20	123/23 (σ_1) (post-folding)
		veins associated to joints	12	123/08 (σ_1) (post-folding)
9 - Wadi Ghul	Natih Fm	veins	18	296/05 (σ_1) (post-folding)

Gomez-Rivas et al., Table 3

(this study)	structures (Hilgers and others, 2006)	structures (Holland and others, 2009a,b)	main tectonic events and large-scale structures; Breton and others (2004); Filbrandt and others (2006); Fournier and others (2006)
#1 - early veins and stylolites Alternatively, *#3* could have also formed here	*V1* - stylolite veins *V2* - bedding-normal veins	*d1* - bedding- normal veins	Formed during subsidence. Structures related digenetic to pulling down of continental lithosphere during subduction of Autochthonous, Turonian-Santonian WNW-ESE normal faults in Block 6
#2 - top-to-the-South layer-parallel shearing		*d2* - bedding-parallel structures (top-to-S)	Ophiolite and Hawasina obduction (top-to-S sense of shear), Mid Turonian-Late Santonian
#3 - normal (dip-slip) to oblique-slip faults & veins	*V5 + V6* - normal faults & associated veins	*d3* - normal faults	Pre-exhumation, and exhumation of the Autochthonous, Early to Mid Campanian Alternatively, Turonian-Santonian, if faults #3 correlate with WNW-ESE normal faults in Block 6
#4 - top-to-the-Northeast layer-parallel veins and cleavage	*V3* - pinch-and-swell veins *V4* - bedding-parallel veins	*d2* - structures parallel to bedding (top-to-N layer-parallel veins)	Exhumation of the Autochthonous. Formation of regional cleavage (top-to-N or -NE sense of shear), ramps, bed-parallel shearing. Campanian
#5 - strike-slip faults and veins (NW-SE-oriented σ_1) Possible dip-slip fault movements	reactivation of *V5+V6* as strike-slip?		Exhumation of the Autochthonous. Formation of large-scale strike-slip faults in Block 6 (Campanian). Limited uplift and erosion. India moved N: oblique transpression between Arabia and Indian Plates during Late Campanian-Mid Eocene. Transgression of tertiary sequence. Folding of Nakhl anticline. NW-SE faults can have dip-slip movement at this time.
#6 - strike-slip faults and veins (E-W-oriented σ_1) Possible dip-slip fault movements	reactivation of *V5+V6* as strike-slip?		General uplift. Late Oligocene-Middle Miocene E-W faults can have dip-slip movements
#7 - strike-slip veins (N-S to NE-SW-oriented σ_1)	reactivation of *V5+V6* as strike-slip?		Miocene-Pliocene. Compression phase recognizable in Neo-Autochthonous units NNE-SSW transpression. Uplift and erosion. Pliocene. Possibly synchronous with N-S compression and transpression (*#7*)
#8 - folding (doming)	reactivation of *V5+V6*? *V7* - veins in late thrust faults?		
#9 - joints		*d4* - uncemented/partly cemented joints	Pliocene – Holocene?